

**EFFECT OF TeO<sub>2</sub> ON THE RADIATION SHEILDING  
PERFORMANCE OF POTASSIUM BORO TELLURITE  
GLASSES**

Submitted by

**RAFIA MARIYAM ABDULAZEEZ**

**Reg. No: AIAWMPH008**

In partial fulfillment of the requirement for the award of the Degree of

**MASTER OF SCIENCE IN PHYSICS**

**UNIVERSITY OF CALICUT**



**M.E.S. ASMABI COLLEGE, P VEMBALLUR**

Affiliated to the University of Calicut

Under the guidance of

**Dr. Naseer K.A**

**Asst. Professor,**

**PG & Research Department of Physics**

**Farook College (Autonomous), Kozhikode**

**APRIL 2024**



**Post Graduate & Research Department of Physics  
Farook College (Autonomous), Calicut**

**CERTIFICATE**

This is to certify that the project work entitled “**Effect of TeO<sub>2</sub> on the Radiation Shielding Performance Of Potassium Boro Tellurite Glass**” submitted by **Ms.RAFIA MARIYAM ABDULAZEEZ (AIAWMPH008)** at Farook College (Autonomous), Calicut, is the work done under my supervision during the period 2022-2024, in partial fulfillment of requirements for the award of the degree of Master of Science in Physics, MES Asmabi College, P Vemballur. She has not submitted the present work to any other university or institute for the award of a degree or diploma.

Dr. Naseer K.A.  
Assistant Professor  
Department of Physics  
Farook College (Autonomous),  
Kozhikode



**Department of Physics,  
M.E.S. Asmabi College, P Vemballur – 680671**

### **CERTIFICATE**

Certified that the project report entitled “**Effect of  $\text{TeO}_2$  on the Radiation Shielding Performance Of Potassium Boro Tellurite Glass**” submitted by **Ms.RAFIA MARIYAM ABDULAZEEZ (AIAWMPH008)** at Farook College (Autonomous), Calicut, under the guidance of Dr. K.A. Naseer, in partial fulfillment of the requirement for the award of the degree of Master of Science in Physics from University of Calicut and the same has been submitted to M.E.S. Asmabi College, P. Vemballur.

Dr. Ebitha Eqbal  
Assistant Professor & HoD,  
Department of Physics  
M.E.S Asmabi College  
P. Vemballur

**EFFECT OF TeO<sub>2</sub> ON THE RADIATION SHEILDING  
PERFORMANCE OF POTASSIUM BORO TELLURITE  
GLASSES**

Submitted by

**Ms. RAFIA MARIYAM ABDULAZEEZ**

**(AIAWMPH008)**

The project presentation / viva voice held on ..... At M.E.S. Asmabi  
College, P. Vemballur, is evaluated and approved by

**External Examiners:**

1.

2.

## **DECLARATION**

I hereby declare that the project work entitled “**Effect of TeO<sub>2</sub> on the Radiation Shielding Performance Of Potassium Boro Tellurite Glass**” submitted to the Department of Physics, M.E.S. Asmabi college, P. Vemballur, affiliated to the University of Calicut, in the partial fulfillment of the requirement for the award of the degree of Master of Science in Physics is a record of the original work done by me during 2022-2024 under the guidance of **Dr.NASEER K.A**, Assistant Professor, Department of Physics, Farook College, Calicut. This project report is not part of any other Calicut University or other university projects.

Place:

**Ms. RAFIA MARIYAM ABDULAZEEZ**

Date:

**AIAWMPH008**

## ACKNOWLEDGEMENT

First and foremost, I thank the Almighty with a humble heart for his abiding presence, which sustained me throughout this project.

It gives me great pleasure to express my deep sense of gratitude and indebtedness to my guide, **Dr. Naseer K.A.**, Assistant Professor of Physics,

Post Graduate & Research Department of Physics, Farook College (Autonomous), Calicut, for his valuable guidance, scholarly advice, and constant encouragement throughout the project. I am highly obliged to him for providing me with this opportunity to carry out his ideas and work during my project and helping me to achieve its successful completion.

I express my gratitude to our former HoD **Dr. Sheena P A**, present HoD **Dr. Ebitha Eqbal**, Assistant Professor, M E S Asmabi College, P. Vemballur and **Dr. A Biju**, the Principal of M E S Asmabi college. P. Vemballur for the support and guidance.

I am immeasurably thankful to my **Family, Teachers and Friends** for their love and constant support throughout the work.

Finally, I would like to thank everybody who was important to the successful realization of this work as well as expressing my apology that I could not mention personally one by one.

## **ABSTRACT**

The current study intended to analyze radiation shielding properties of Boro Tellurite Pottasium glass systems in compositions of  $(70-x)$   $B_2O_3+xTeO_2+15K_2O+15MgO$  (where  $x$  is 0, 10, 20 30, and 40 wt%), labeled as 00BTK, 10BTK, 20BTK, 30BTK, 40BTK prepared by melt quenching technique. The theoretical values of radiation shielding properties were computed by the Phy-X program in the energy range 0.015 MeV–15 MeV. Radiation attenuation parameters such as the mass attenuation coefficients ( $\mu_m$ ), half value layer (HVL), tenth value layer (TVL), mean free path (MFP), and equivalent atomic number ( $Z_{eq}$ ), were calculated to ascertain the radiation shielding properties of the selected glasses. Structural features are also discussed. The xBTK glass with 40 wt%  $TeO_2$  is superior to transparent gamma-ray shielding. The investigation was carried out to explore the advantages of xBTK glasses in different radiation shielding applications.

## **CONTENTS**

<b>CHAPTER 1 GENERAL INTRODUCTION</b>	<b>12</b>
<b>1.1 GLASSES-AN OVERVIEW</b>	<b>14</b>
<b>1.2 METHODS OF GLASS PREPARATION</b>	<b>15</b>
<b>1.3 MELT QUENCHING METHOD</b>	<b>15</b>
<b>1.4 RADIATION AND RADIOACTIVE DECAYS</b>	<b>17</b>
<b>CHAPTER 2 EXPERIMENTAL METHODS AND MATERIALS</b>	<b>22</b>
<b>2.1 FABRICATION OF GLASSES</b>	<b>22</b>
<b>2.2 METHODS OF DATA COLLECTION</b>	<b>23</b>
<b>2.3 MEASUREMENT OF STRUCTURAL PROPERTIES</b>	<b>25</b>
<b>2.4 MEASUREMENT OF RADIATION SHIELDING PROPERTIES</b>	<b>28</b>
<b>2.5 RADIATION SHIELDING PARAMETERS</b>	<b>31</b>
<b>CHAPTER 3 RESULT AND DISCUSSION</b>	<b>36</b>
<b>3.1 PHYSICAL PROPERTIES</b>	<b>36</b>
<b>3.2 STRUCTURAL CHARACTERIZATION</b>	<b>42</b>
<b>3.3 RADIATION SHIELDING PROPERTIES</b>	<b>43</b>
<b>CHAPTER 4 CONCLUSION</b>	<b>51</b>
<b>CHAPTER 5 FUTURE PROSPECTS AND PRESENTATION</b>	<b>52</b>
<b>5.1 FUTURE SCOPE</b>	<b>52</b>
<b>5.2 ADVANTAGES AND DISADVANTAGES</b>	<b>53</b>
<b>CHAPTER 6 REFERENCE</b>	<b>54</b>



## LIST OF FIGURES

<b>Figure 2.1 Flow chart of the PSD online software</b>	<b>29</b>
<b>Figure 2.2 The main screen interface of the PSD online software</b>	<b>31</b>
<b>Figure 3.1 XRD Analysis</b>	<b>54</b>
<b>Figure 3.2 TVL of 00BTK, 10BTK, 20BTK, 30BTK, 40BTK</b>	<b>43</b>
<b>Figure 3.3 Variation of MFP v/s Gamma Energy</b>	<b>45</b>
<b>Figure 3.4 Half Value Layer of glasses at 3 and 4 MeV</b>	<b>45</b>
<b>Figure 3.5 Ratios V/S Gamma energy</b>	<b>47</b>
<b>Figure 3.6 Z<sub>eq</sub> V/S Gamma energy</b>	<b>48</b>
<b>Figure 3.7 MAC V/S Gamma Energy variation</b>	<b>50</b>

## LIST OF TABLES

**Table 3.1 Composition, corresponding glass code, density ( $\rho$ ), and average molecular weight ( $M_{av}$ ) of Pottasium Boro Tellurites glasses.**

Error! Bookmark not defined.

**Table 3.2 Structural properties of xBTK glasses** **41**

**Table 3.3 Ionic character factor (Ic%) and covalent factor (Cc%) of Pottasium Boro Tellurite glasses**

Error! Bookmark not defined.

## LIST OF SYMBOLS AND ABBREVIATIONS

SYMBOLS	ABBREVIATIONS
$\rho$	Density of the substance
Nd	Refractive Index
$\lambda$	Wavelength
Mav	Average Molecular Mass
Vm	Molar volume
Rm	Molar Refractivity
Dd (Te)	Distribution Density of Tellurium
r(Te-Te)	Tellurium-Tellurium separation
Vo	Molar Volume of Oxygen
M	Metallization criterion
Eg	Optical Band gap
$\beta$	Two photon absorption coefficient
R	Reflection losses
$\Lambda$	Optical Basicity
Na	Avogadro Number
$\chi_{opt}$	Optical electronegativity
$\alpha_m$	Molar polarizability
Cc	Covalent factor
Ic	Ionic factor
Io	Intensity of incident photon
I	Intensity of attenuated photon
Tm	Mass thickness
t	Thickness of the material
$\mu_m$	Mass attenuation coefficient
$\mu$	Linear attenuation coefficient
Zeq	Equivalent Atomic Number
Neff	Effective electron density

# CHAPTER 1

## INTRODUCTION

### GENERAL INTRODUCTION

Life is but a continuous process of energy conversion and transformation. The accomplishments of civilization have largely been achieved through the increasingly efficient and extensive harnessing of various forms of energy to extend human capabilities and ingenuity. Energy is similarly indispensable for continued human development and economic growth. Providing adequate, affordable energy is essential for eradicating poverty, improving human welfare, and raising living standards worldwide. And without economic growth, it will be difficult to address environmental challenges, especially those associated with poverty. But energy production, conversion, and use always generate undesirable by-products and emissions at a minimum in the form of dissipated heat. Energy cannot be created or destroyed, but it can be converted from one form to another. The same amount of energy entering a conversion process, say, natural gas in a home furnace, also leaves the device some 80–90 percent as desirable space heat or warm water, the rest as waste heat, most through the smokestack. Although it is common to discuss energy consumption, energy is transformed rather than consumed. What is consumed is the ability of oil, gas, coal, biomass, or wind to produce useful work. Among fossil fuels the chemical composition of the original fuel changes, resulting in by-products of combustion, or emissions. Due to this emission leads to environmental pollution causing global warming and more threatening climate change, hence this has become a global issue today and this fact reinforces the necessity of enhancing nuclear energy capacity. According to International Atomic Energy Agency (IAEA), “To address the challenges posed by climate change, and to achieve the goals established in the 2015 Paris Agreement, nuclear power has been identified to have great potential to contribute to the 1.5°C climate change mitigation target”

Climate change has become a problem in many countries' day by day, and this fact confirms the necessity of using nuclear power plants, which are a source of alternative energy. Although the Three Mile Island, Chernobyl and Fukushima Daiichi nuclear accidents cause concern over these plants, over the past 60 years, great advances have been provided in waste management using nuclear power plants. To

dispose of these wastes, many studies have been conducted in most countries for a long-term and reliable solution.

Nuclear waste management is quite a difficult process since high radioactive isotopes are produced in the existing power plants. These radioactive isotopes have longevity and risk of toxicity. Most countries have been developing various strategies for waste management and control. They keep on conducting studies to produce durable and strong materials. Besides natural radiation, it is vital to use highly protective materials in waste management to minimize the environmental risks of ionizing radiation produced by human hands. The most significant impacts of ionizing radiation can be seen in this high radiation waste. Therefore, it is very crucial the correct management of this high radiation waste. International simple glass (ISG) can be produced as an alternative to traditional methods. According to recent studies in literature, materials which are relatively lightweight, accessible, non-toxic, cheap, have a high thermal resistance of shielding performance, improving the known disadvantages of concrete. Concrete and other traditional materials were used as shielding material for many years to make the environment safe and protect workers from hazardous radiation. Concrete has been widely used as a radiation shielding material as it is widely available, is of extremely low cost when compared to other shielding materials and can be effortlessly molded into any desired shape. Despite these many advantages there are some disadvantages also associated with the use of concrete like it is not transparent to visible light which limits one to see through it. Secondly, on prolonged exposure to radiation, its mechanical strength gets reduced. One of the prominent structures in these studies is glass or glassy materials, which have many advantages in terms of radiation shielding. These materials, especially due to their superior features such as transparency, attenuating gamma photons, and ease of use in new generation technological fields, attract a lot of attention among alternative and innovative glassing material. Glass systems have some promising properties in terms of not only radiation shielding capability but also being visible to light, which makes it possible to observe and control the experimental condition. Also, with the help of vitrification (The process of converting liquid radioactive and chemical waste into a solid, stable glass, eliminating environmental risks) process glass plays an important role in reducing the hazards of different types of waste by keeping them chemically stable for a long time.

Now a days heavy metal glasses are proving to be a potential candidate as a substitute for conventional radiation shielding material like concrete. Lead is a heavy metal usually used for this purpose, but its use is often not encouraged due to its toxic and hazardous nature. In this study different compositions of Boron Tellurium Pottasium glasses doped with different amount of Boron are studied for radiation shielding purposes based on assessing different shielding parameters.

### **1.1 GLASSES-AN OVERVIEW**

Glass has transformed the world like no other material. However, people usually ignore it. Without glass, the world would be bizarre. It's in the eyeglasses on our face, the light bulbs in our room and the windows that let us see outside. Glasses have some exclusive characteristics which are not found in other materials. The combination of hardness and transparency at room temperature along with adequate strength and exceptional corrosion resistance make glasses crucial for many sensible applications. Many attempts to define a glass have been made in the last few decades with contrasting degrees of success. However, a precise definition is still imminent, and this should consider the relationship of glasses with other amorphous solids. Mackenzie's definition is enough for the present discussion and is used as a working principle for the current research. According to him, glass is any isotropic substance (organic or inorganic) in which the three-dimensional atomic periodicity is absent, and it has a viscosity greater than  $10^{14}$  poise. The rapid cooling procedure employed in the glass production results in a "freeze up" of the liquid disorder. The resultant lack of periodicity of the primary structural units distinguishes glass from crystal. Debye has documented that a regular crystal environment is not necessary for X-ray diffraction. While crystals generate sharp lines in X-ray powder diffraction, amorphous materials such as liquids and glasses, in general, make several diffuse bands. This is because the well-defined lattice parameters, required for sharp diffraction lines, are absent in glasses.

There are several advantages for glass materials over crystalline materials in many optical device applications. However, glass, an inorganic solid material that is usually transparent or translucent as well as hard, brittle, and impervious to the natural elements. Glass has been made into practical and decorative objects since ancient times, and it is still very important in applications as disparate as building construction, housewares, and telecommunications. It is made by cooling molten

ingredients such as silica sand with sufficient rapidity to prevent the formation of visible crystals. The varieties of glass differ widely in chemical composition and in physical qualities. Most varieties, however, have certain qualities in common. They pass through a viscous stage in cooling from a state of fluidity; they develop effects of color when the glass mixtures are fused with certain metallic oxides; they are, when cold, poor conductors both of electricity and of heat; most types are easily fractured by a blow or shock and show a conchoidal fracture; and they are but slightly affected by ordinary solvents but are readily attacked by hydrofluoric acid. Boro-tellurite glasses have recently been attracting the attention of several researchers as a tremendous optical device and shielding material. Boro Tellurite glasses were studied impressively and widely due to their better physical properties like high thermal stability, low melting point, good, rare earth ions solubility, good mechanical strength, chemical durability, high dielectric constant, lower phonon energy and best transmission in the visible and IR wavelength regions.

## **1.2 METHODS OF GLASS PREPARATION**

The properties of the glasses are controlled by certain factors like the chosen composition, preparation methods, glass structure, photosensitive nature, thermal, mechanical, and chemical durability etc., Numerous methods can be adopted for the synthesis of amorphous materials. The following methods are detailed by Elliot and Zarzycki.

- |                                 |                              |
|---------------------------------|------------------------------|
| 1) Melt -quenching              | 7) Electrolytic deposition   |
| 2) Thermal evaporation          | 8) Chemical reaction         |
| 3) Sputtering                   | 9) Reaction amorphization    |
| 4) Glow-discharge decomposition | 10) Irradiation              |
| 5) Chemical vapour deposition   | 11) Shockwave Transformation |
| 6) Gel-desiccation              | 12) Shear amorphization      |

## **1.3 MELT QUENCHING METHOD**

Melt-quenching is the traditional technique of glass making and includes mixing of ingredients, heating up to a temperature usually higher than 1300 °C and quenching of the glass melt to obtain a glass frit (Gerhardt and Boccaccini, 2010). The melt quenching technique was the only technique available for the fabrication of semiconductor-doped glasses. In particular, it was used by commercial glass makers (e.g., Schott, Corning, Hoya, etc.) for the fabrication of sharp cutoff optical filters.

The main breakthrough in the investigation of the nonlinearities of this kind of glasses was in 1983, when Jain and Lind observed their very high third-order susceptibility. But some of the nonlinear properties of these glasses were known before. In 1964, Bret and Gires used the Schott glass RG715 as a saturable absorber for a ruby laser.

Even if the melt quenching technique is very well controlled and widely used for the fabrication of glasses and glass filters, it is not optimized for the specific demands of semiconductor-doped glasses for nonlinear optics. The main drawbacks are the rather impure semiconductor composition and the surface imperfection of the nanoparticles. However, melt quenching remains a valuable glass fabrication technique, and recent research has shown that its potential is not yet totally explored. Moreover, one has to distinguish between commercial glass filters and “research” samples that are optimized for the specific needs of this field. The problem that thin films cannot be produced by this technique can be overcome by using (for example) ion exchange to realize integrated optics devices.

Glass can be manufactured effectively by the melt quenching technique in which the following step by step procedures are adopted generally

1. Formation of batch material
2. Melting
3. Shaping
4. Annealing and
5. Finishing

### **1.3.1 Formation of batch material**

The selected raw materials are to be weighed accurately in required proportions before they are mixed. The mixing should be done using an agate mortar or any other mixing aid, till we get a uniform mixture. The adequately mixed uniform mixture is known as a batch, which will be used for the melting in a furnace. Proper amount in wt% of chemicals in powder/crystal form are weighed using a digital balance having a sensitivity of  $\pm 0.0001\text{g}$ ; 15 g batches of selected composition are used in each work of the current study.

### **1.3.2 Melting**

In the present study, the batch is kept in a porcelain crucible and then melted using an electric furnace. The melting temperature and the duration of heating are depending on the selected composition.



### **1.3.3 Shaping**

One can give a suitable shape or form to the molten glass in this stage. There are different methods of fabrication, such as, blowing, casting, drawing, pressing, rolling, and spinning according to the purpose of preparation. Among these, the casting technique is used to fabricate the glass samples in this study. By keeping a preheated brass mould in an electrical furnace, and pouring the molten mixture into it, one can obtain the particular shape. The glass samples in this research are made as rectangular slabs.

### **1.3.4 Annealing**

The glass is to be cooled down at a temperature which is  $1/3^{\text{rd}}$  of the melting temperature for a longer time. This process is known as annealing. The annealing of glass is a very crucial process. If the glass is cooled quickly, the upper layer of the glass cools down first since glass is a bad conductor of heat. The inner portion remains relatively hot. This makes a state of strain. Hence, such glasses are easy to break even under slight shocks or disturbances. Among the flue treatment and the oven treatment, oven treatment was chosen to anneal the current samples.

### **1.3.5 Finishing**

After the annealing process, the prepared glasses are allowed to reach room temperature gradually on its own course of time. Finally, finishing is essential to obtain a clear polished transparent glass which is used for further optical studies. Finishing is usually carried out by cleaning, washing, grinding, polishing, cutting, sand blasting, enamelling and gapping. In this process, the glass samples are polished using various grades of silicon carbide powder for obtaining parallel, smooth and clear surface for experiment. The thickness of glass specimens is measured using a digital micrometer gauge.

## **1.4 RADIATION AND RADIOACTIVE DECAYS**

It is found that a few naturally occurring substances consist of atoms which are unstable that is, they undergo spontaneous transformation into more stable product atoms. Such substances are said to be radioactive and the transformation process is known as radioactive decay. Radioactive decay is usually accompanied by the emission of radiation in the form of charged particles and gamma rays.

Radiation has been a source of fascination and concern ever since Wilhelm Konrad Röntgen discovered X-rays on 8 November 1895. Over the years, health workers as well as the public have been concerned about medical uses of X-rays, the presence of radon in buildings, radioactive waste from nuclear power stations, fallout from nuclear test explosions, radioactive consumer products, microwave ovens, and many other sources of radiation. Most recently, the tragic accident at the Chernobyl nuclear power station in the USSR, and the subsequent contamination over most of Europe, has again wakened interest and concern and also reminded us about a number of misconceptions about radiation.

Radiation which has enough energy to remove electrons from an atom is known as the ionizing radiation. The DNA may possibly be damaged by the ionizing radiation, under a huge exposure or even lead to form cancer. As radiation is harmful to human health, it should be protected. The most significant way to get protected from radiation is shielding. The commonly used shielding materials are lead and heavy materials. Currently, new products for these purposes are being developed and started to use in radiation shielding.

#### **1.4.1 Gamma Matter Interaction**

Interaction of  $\gamma$ -rays with matter could produce charged particles like positrons and electrons at relativistic speed. Depending upon the interacting particle/field in the matter,  $\gamma$ -rays can interact with many processes. Various combinations of interacting particle/field give twelve processes of photon interaction. Based on the probability of existence, there are three dominant photon interaction processes. All kinds of radiation interact differently with the matter. The interaction process relies on the nature of the radiation, its capability to penetrate and ionize matter. The interaction of Gamma rays with matter happens in three modes (Photoelectric effect, Compton scattering and Pair production) as described below. A few Gamma-ray photons may also pass through the matter even without interacting with it. The Gamma-ray photons are removed from the beam by absorption or scattering and get attenuated exponentially.

##### **Photoelectric effect**

The interaction process when an incoming Gamma-ray photon interacts with the atom and transfers whole of its energy to a bound atomic electron and the electron gets knocked out from the atom, is called as photoelectric effect and the emitted

electron is called the photoelectron. The energy of the incoming Gamma-ray photon must be higher than the binding energy of the photoelectron which is used in overcoming the binding energy of the photoelectron and rest of its energy is imparted to the photoelectron. Thus, the entire energy of Gamma-ray photon is absorbed and it vanishes completely. On emission of the photoelectron, the atom gets ionised with a vacancy in one of its shells. When the vacancy is in one of the inner shells, then it is promptly filled by higher shell electrons, thus emitting characteristic X-rays. These X-rays may get absorbed or can also escape the medium. If these X-rays have energy more than the binding energy of higher-shell electrons, then the X-rays may be absorbed and it results in further ejection of electrons, known as Auger electrons. The cross-section for photoelectric absorption is depending on the energy of Gamma-ray photons as  $E^{-3.5}$ . It implies that probability of photoelectric effect is greater at lower energies.

### **Compton scattering**

Compton scattering (or the Compton effect) is the quantum theory of high frequency photons scattering following an interaction with a charged particle, usually an electron. Specifically, when the photon hits electrons, it releases loosely bound electrons from the outer valence shells of atoms or molecules. When an incoming Gamma-ray photon interacts with the atom and transfers a part of its energy to a free or weakly bound atomic electron, the photon gets scattered accompanied by a drop in its energy and the electron gets knocked out from the atom, the interaction process is known as Compton scattering. Compton scattering occurs when the energy of the Gamma photon is much higher as compared to the binding energy of the electrons. A part of the energy of incident Gamma-ray photon is transferred to the ejected electron and the scattered photon travels with the other part. In this way, only a part of the energy of Gamma-ray photon is absorbed and it does not disappear entirely. After the interaction, the scattered Gamma-ray photon further propagates in the material medium. It can interact with another atom and get fully absorbed by photoelectric effect. There is also a possibility of multiple Compton scattering. The photon may also escape from the medium. The electron also loses its energy as a Beta electron by ionization. The cross-section for Compton scattering varies slowly with the energy of Gamma-ray photons as  $E^{-1}$ . It implies that probability of Compton scattering is greater at intermediate energies. The Compton scattering is dominant in the intermediate

energy region (150 keV to 5 MeV). The cross-section for Compton scattering is least dependent on the atomic number of the absorber material as  $Z^1$ . This is also directly related to number of electrons in the outermost shell i.e. the electron density.

### **Pair production**

When an incoming Gamma-ray photon comes under the strong electromagnetic field of a nucleus, its energy gets converted to the mass of an electron and a positron pair, the interaction process is known as pair production. The energy of the incoming Gamma-ray photon must be higher than 1.022 MeV (twice the rest mass of electron) for pair production to occur. The excess amount of Gamma photon energy above 1.022 MeV is imparted to the electron and positron as kinetic energies. In this process, whole of the energy of Gamma-ray photon is absorbed and it disappears fully. After the interaction, the positron and electron traverse in the medium and lose energy by ionization and excitation processes. When the positron stops along its path, it combines with a nearby electron and gets annihilated, resulting in the production of two Gamma-ray photons of energy 511 keV each, in opposite directions. These two Gamma-ray photons may further interact with the medium and result in photoelectric or Compton scattering or may also escape from the medium. The cross-section for pair production process depends on Gamma-ray photon energy as  $\log E$ . With increase in photon energy, probability of pair production increases. This process is dominant in high energy region ( $> 5$  MeV). The cross-section for pair production process also depends on the atomic number ( $Z$ ) of the absorber material as  $Z^2$ . This interaction becomes more important for high atomic number absorber materials.

Apart from these three major interaction processes, coherent scattering or the Rayleigh scattering can also happen at low energies in which the Gamma-ray Introduction to Nuclear Radiations photons get scattered in the presence of field of bound electrons. The atoms of the matter neither get ionized nor excited. There is also a possibility of absorption of the Gamma-ray photon by the atomic nucleus which may give rise to photonuclear reactions. The nucleus gets excited and then results in either the emission of protons or neutrons by  $(\gamma, p)$  and  $(\gamma, n)$  reactions.

### **1.4.2 Shielding**

Radiation shielding is the practice of placing a barrier between a source of radiation and an area or person to absorb the radiation energy. This protective measure ensures safety by reducing exposure to harmful ionizing radiation. The  $\gamma$ -ray shielding

materials require homogeneous density and composition to effectively attenuate radiation. Additionally, the thickness of the shielding material should be adequate to absorb the radiation to a safe level. Mass attenuation coefficient, MAC ( $\mu_m$ ), linear attenuation coefficient, LAC ( $\mu$ ), mean free path (MFP), effective atomic number ( $Z_{\text{eff}}$ ), half-value layer (HVL), tenth value layer (TVL), electron density ( $N_e$ ) and buildup factor (energy absorption buildup factor, EABF and exposure buildup factor, EBF) are the fundamental quantities which determine the scattering and the absorption of radiation. MAC (Mass Attenuation Coefficient) is a measure of the number of photons interacted (may be scattered or absorbed) with the interacting material, expressed in  $\text{cm}^2/\text{g}$ . A higher MAC indicates a greater probability of photon interaction, resulting in better attenuation (absorption or scattering) of radiation. MFP (Mean Free Path) denotes the average distance a photon can travel in a material between two consecutive interactions. For radiation shielding samples of similar thickness, a material with a lower MFP value at a specific photon energy provides better shielding against  $\gamma$ -rays. Electron density ( $N_{\text{eff}}$ ) is the number of electrons per unit mass of the material. If the  $N_{\text{eff}}$  is high, the  $\gamma$ -ray shielding material is better as it provides a higher probability of photon interaction with the material. Radiation protection efficiency (RPE) is the efficiency of a shielding material to attenuate high energy incident radiations. Higher values of RPE indicate larger shielding efficiency. Equivalent atomic number ( $Z_{\text{eq}}$ ) The equivalent atomic number represents the average atomic number of the atoms surrounding a central metal ion in a coordination complex. The equivalent atomic number influences how effectively the glass attenuates ionizing radiation (such as X-rays or gamma rays). Glasses are favored as radiation shielding materials due to several advantages: they are stable in both air and water, transparent to visible light, capable of being manufactured in large volumes, and importantly, can be produced with high densities. Glasses doped with heavy metal oxides are particularly utilized for radiation shielding purposes. In this work Pottasium glass system is used as a shielding material.

## **CHAPTER 2**

### **EXPERIMENTAL METHODS AND MATERIALS**

#### **2.1 FABRICATION OF GLASSES**

In the process of preparing glasses for specific applications, meticulous attention is devoted to the composition and selection of raw materials. High-purity analytical-grade chemicals, sourced from Sigma Aldrich for their reliability and consistency at 99.99% purity, are meticulously weighed and combined in appropriate proportions using an agate mortar to ensure uniformity, resulting in what is termed as a "batch." Utilizing batches weighing 15 grams and comprising selected compositions, the subsequent steps are carefully executed.

The batch is then placed into a porcelain crucible and subjected to melting in an electric furnace at 980°C for two hours. Periodic stirring of the molten mixture is undertaken during this process to achieve homogeneity. Following melting, the molten mixture is poured into a brass mould, maintained at 300°C in an annealing furnace, for approximately 8 hours. This annealing process serves to improve thermal strain and eliminate bubbles while improving the mechanical strength and overall quality of the glass.

Upon completion of annealing, the furnace is allowed to gradually cool to room temperature, facilitating the slow cooling of the glass. The resultant glasses are subsequently polished to attain a smooth and flat surface, enhancing optical measurements. For the specific study at hand, high-purity analytical-grade chemicals, including B<sub>2</sub>O<sub>3</sub>, TeO<sub>2</sub>, K<sub>2</sub>O, and MgO, provided by Sigma Aldrich, are employed. Utilizing the conventional melt-quenching technique, glasses doped with tellurite in Pottasium Boro Tellurites compositions are fabricated.

Nuclear shielding glass is a type of glass that can absorb or block harmful radiation, such as gamma rays, X-rays, and neutrons. Nuclear shielding glass is usually made by adding heavy metal oxides, such as lead oxide, bismuth oxide, or erbium oxide, to a borate glass base. These metal oxides increase the density, refractive index, and optical band gap of the glass, which enhance its shielding properties. Nuclear shielding glass can be prepared by melting the raw materials at high temperatures and then cooling them rapidly to form a glassy solid. The composition, structure, and properties of nuclear shielding glass can be varied by

changing the type and amount of metal oxides, alkali modifiers, and other additives. Nuclear shielding glass has applications in medical, industrial, and nuclear fields, where it can protect people and equipment from radiation exposure.

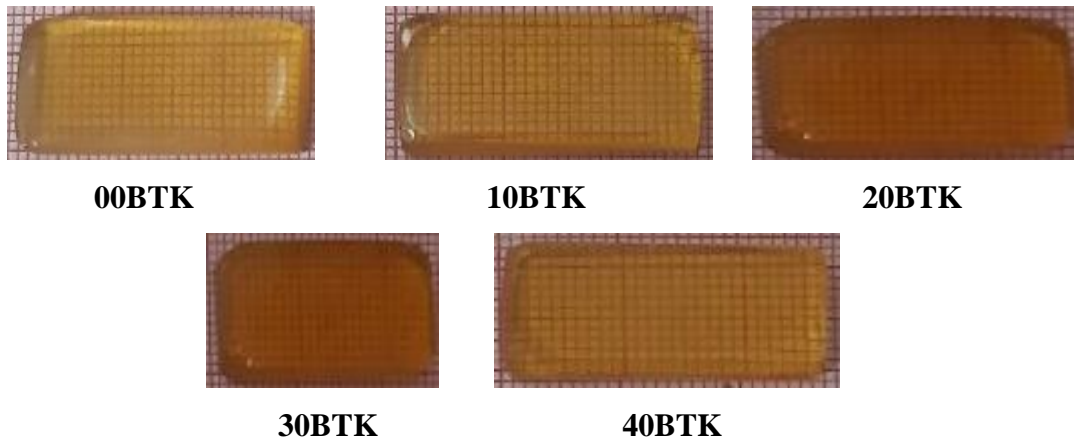


**Figure 1.1:** Prepared Glass samples

This paper examines the role of Tellurium in the structural and radiation shielding properties of glasses with compositions represented as  $(70-x)\text{B}_2\text{O}_3+x\text{TeO}_2+15\text{K}_2\text{O}+15\text{MgO}$ , where  $x = 0, 10, 20, 30,$  and  $40$  wt% and different glass codes are assigned for each composition. In this study five different compositions of Potassium Boro Tellurite glass samples containing different amount of boron are selected to extensively investigate their capacity to be used as radiation shield.

## 2.2 METHODS OF DATA COLLECTION

- **Density,  $\rho$  (g/cm<sup>3</sup>)**

The densities of the glasses have been determined by employing the Archimedes principle, where-in xylene is used as an immersion liquid with a density of 0.865. The glass was weighed in air ( $W$ ) and xylene liquid ( $W_1$ ), at room temperature using a monopan balance. The density ( $\rho$ ) is calculated using the equation,

$$\rho = \frac{W}{W - W_1} \times 0.865 \quad 0.1$$

Using the measured thickness, refractive index, and the density of the glass samples various physical, structural, and elastic properties are calculated following the corresponding equations. Armed with the density value, researchers can explore various physical, structural, and elastic properties of the glass sample. These properties include refractive index, mechanical strength, and other material characteristics.

- **Thickness, l (mm)**

The thickness (l) of the studied glasses was measured after finishing the polishing using a screw gauge having least count value of  $\pm 0.01$  mm.

- **Refractive index, nd**

The refractive index of the prepared glasses is measured using Abbe's refractometer ATAGO NAR-4T with a light source of wavelength  $\lambda = 589.3$  nm and mono bromonaphthaline as the contact liquid. The measurement is made at room temperature. The range of the specified model is 1.4700-1.8700 and can be measured with an accuracy of  $\pm 0.0002$ .

A reference prism with a refractive index of 1.6 is used for the primary adjustments of the Abbe's refractometer. After the calibration, the glass is placed on the optical bench of the refractometer. The contact liquid, mono bromonaphthaline helps to avoid the air column in between the surfaces. It has a refractive index of 1.658 which will prevent the interference during the refractive index measurement for the specimen. The glass is then illuminated with the light source.

- **Average molecular mass**

The average molecular mass, also referred to as molar mass or molecular weight, quantifies the mass of a molecule relative to the unified atomic mass unit (u). This value is expressed in grams per mole (g/mol).

To calculate the average molecular mass, we follow this equation: The average molecular mass, also referred to as molar mass or molecular weight, quantifies the mass of a molecule relative to the unified atomic mass unit (u). This value is expressed in grams per mole (g/mol). To calculate the average molecular mass, we follow this equation:

$$M_{av} = \sum_i (n_i \times m_i) \quad 0.2$$

Where,  $n_i$  represents the number of atoms of each element in the compound's chemical formula,  $m_i$  represents the atomic mass of each element in unified atomic mass units (u).

- **Molar Volume,  $V_m$  ( $\text{cm}^3/\text{mol}$ )**

The molar volume, denoted as **Vm**, represents the volume occupied by **one mole** of a substance; the molar volume is the ratio of the volume occupied by a



substance to the amount of that substance. The molar volume of each glass is obtained from the equation:

$$V_m = \frac{M_{av}}{\rho} \quad 0.3$$

- **Molar refractivity  $R_m$  ( $\text{cm}^3/\text{mol}$ )**

The molar refractivity, symbolized as **Rm**, quantifies how effectively a substance can bend or refract light. It's a property related to the interaction of light with matter. The equation for calculating molar refractivity  $R_m$  is:

$$R_m = V_m \times \left( \frac{n_d^2 - 1}{n_d^2 + 2} \right) \quad 0.4$$

### 2.3 MEASUREMENT OF STRUCTURAL PROPERTIES

- ❖ **Distribution density of Tellurium,  $D_{d(\text{Te})}$  ( $\text{m}^{-2}\text{mol}^{-1}$ )**

The density distribution of tellurium refers to the spatial arrangement or concentration of tellurium atoms within a material or substance. It is determined by the formula:

$$D_{d(\text{Te})} = \frac{r(\text{Te} - \text{Te})}{V_m} \quad 0.5$$

- ❖ **Tellurium-Tellurium separation  $r(\text{Te}-\text{Te})$  (m)**

Tellurium-Tellurium separation refers to the distance or spacing between tellurium atoms within a material or compound. It is a measure of the arrangement of tellurium atoms in a crystal lattice or molecular structure. It is determined by the equation:

$$r(\text{Te} - \text{Te}) = \left( \frac{V_m^{\text{Te}}}{N_A} \right)^{1/3} \quad 0.6$$

$V_m^{\text{Te}}$  is the molar volume of boron and  $N_A$  is the Avagadra Number.

$$V_m^{\text{Te}} = \frac{V_m}{2(1 - X_{\text{Te}})} \quad 0.7$$

- ❖ **Molar Volume of Oxygen, ( $V_o$ ) ( $\text{cm}^3/\text{mol}$ )**

The molar volume of oxygen refers to the volume occupied by one mole of oxygen gas at a specific temperature and pressure. It is measured by the equation:

$$V_o = \frac{V_m}{\sum_i(xn_o)_i} \quad 0.8$$

Where,  $V_m$  is the molar volume,  $x$  is the molar fraction of each component  $i$ , and  $n_o$  is the number of oxygen atoms in each constituent oxide.

❖ **Oxygen Packing Density (OPD)(mol/cm<sup>3</sup>)**

Oxygen packing density refers to the measure of how efficiently oxygen atoms are packed or arranged within a material or substance. The determined using the given equation:

$$OPD = 1000 \times C \times \frac{\rho}{M} \quad 0.9$$

where,  $C$  is the number of oxygen atoms per each composition.

❖ **Metallization Criterion,  $M$**

Metallization criteria refer to the specific requirements or standards that must be met in the process of metallization, which involves applying a thin layer of metal onto a substrate material. These criteria are essential for ensuring the quality, performance, and reliability of the metallized product. Metallization criteria can vary depending on the application, industry standards, and specific requirements of the project. It is calculated by:

$$M = 1 - \frac{R_m}{V_m} \quad 0.10$$

❖ **Optical band gap,  $E_g$  (eV)**

The optical band gap  $E_g$  is the energy difference between the top of the valence band and the bottom of the conduction band in a material. It represents the minimum energy required to promote an electron from the valence band to the conduction band, allowing it to conduct electricity.

The optical band gap is a key parameter in the study of semiconductors, insulators, and other materials, as it influences their optical and electrical properties, including absorption and emission of light, conductivity, and more. It is determined by the equation:

$$E_g = 20\left(1 - \frac{R_m}{V_m}\right)^2 \quad 0.11$$

❖ **Two photon absorption coefficient,  $\beta$  (cm/GW)**

The two-photon absorption coefficient ( $\beta$ ) is a parameter that quantifies the probability of a material undergoing a two-photon absorption process. It is calculated by:

$$\beta = 36.66 - 8.1E_g \quad 0.12$$

❖ **Reflection losses, (R%)**

Reflection losses refer to the portion of incident light that is reflected away at the interface between two different mediums, rather than being transmitted or absorbed by the material. When light encounters a boundary between two mediums with different refractive indices, some of the light may be reflected back into the original medium due to the discontinuity in the refractive index. It is determined by:

$$R(\%) = \left(\frac{n_d - 1}{n_d + 1}\right)^2 \times 100 \quad 0.13$$

❖ **Optical basicity,  $\Lambda$**

Optical basicity indicates how strongly an oxide in a glass composition contributes to its optical properties, such as luminescence, absorption, and emission of light. It is based on the electronic structure of the glass constituents and their ability to participate in electronic transitions that give rise to optical phenomena. It is calculated by the equation:

$$\Lambda_{th} = \sum_i^n x_i \Lambda_i \quad 0.14$$

Where  $\Lambda_{th}$  is the theoretical optical basicity.

The calculated optical basicity is,

$$\Lambda = -0.5\Delta\chi_{glass}^* + 1.7 \quad 0.15$$

$\chi_{glass}^*$  is the optical electronegativity and also it is denoted as  $\chi_{opt}$

$$\chi_{opt} = 9.8e^{-n_d} \quad 0.16$$

❖ **Molar polarizability,  $\alpha_m$**

Molar polarizability refers to the ability of a substance to be polarized by an electric field per mole of the substance. It affects various characteristics such as refractive index. This is determined by the equation:

$$\alpha_m = \frac{R_m}{2.52} \quad 0.17$$

❖ **Ionic factor ( $I_c$  %)**

Ionic bonding occurs when one or more electrons are transferred from one atom to another, resulting in the formation of positively charged ions (cations) and

negatively charged ions (anions). These oppositely charged ions are held together by strong electrostatic forces of attraction, forming an ionic compound. Ionic compounds tend to have high melting and boiling points, are typically soluble in water, and conduct electricity when dissolved or molten. It is calculated by:

$$C_{ionic} = [1 - \exp\{-0.25(\Delta X^2)\}] \times 100 \quad 0.18$$

$\Delta X$  is the difference in the electronegativity of cations and anions.

❖ **Covalent factor ( $C_C$  %)**

Covalent bonding, on the other hand, involves the sharing of electrons between atoms to achieve a stable electron configuration. In a covalent bond, atoms share electron pairs, resulting in the formation of molecules. Covalent compounds tend to have lower melting and boiling points compared to ionic compounds, are often insoluble in water, and do not conduct electricity in their pure state. It is calculated by:

$$C_{covalent} = \exp\{-0.25(\Delta X^2)\} \times 1 \quad 2.19$$

## 2.4 MEASUREMENT OF RADIATION SHIELDING PROPERTIES

In this current work the gamma ray shielding parameters of five glasses having  $(70-x)\text{B}_2\text{O}_3+x\text{TeO}_2+ 15\text{K}_2\text{O}+15\text{MgO}$  (where  $x = 0, 10, 20, 30,$  and  $40$  wt%) compositions were extensively investigated. The Phy-X online platform was utilized for the determination of some essential photon interaction parameters (PIP) such as mass attenuation coefficient (MAC), effective electron density (Neff), Tenth Value Layer (TVL) etc in the energy range 0.015MeV to 15 MeV.

### 2.4.1 Phy-X /PSD : Photon Shielding and Dosimetry Software

User friendly online Photon Shielding and Dosimetry (PSD) software available at <https://phy-x.net/PSD> has been developed for calculation of parameters relevant to shielding and dosimetry. These parameters include linear and mass attenuation coefficients (LAC, MAC), half and tenth value layers (HVL, TVL), mean free path(MFP), effective atomic number and electron density (Zeff, Neff), effective conductivity (Ceff) energy absorption and exposure buildup factors (EABF, EBF). The software can generate data on shielding parameters in the continuous energy region (1 keV-100 GeV). Also, some well-known radioactive sources ( $^{22}\text{Na}$ ,  $^{55}\text{Fe}$ ,  $^{60}\text{Co}$ ,  $^{109}\text{Cd}$ ,  $^{131}\text{I}$ ,  $^{133}\text{Ba}$ ,  $^{137}\text{Cs}$ ,  $^{152}\text{Eu}$  and  $^{241}\text{Am}$ ) along with their energies and some characteristic (K-shell) X-ray energies of Cu, Rb, Mo, Ag, Ba and Tb elements are available in the software and can be selected by the user. Thus, one can obtain the

shielding parameters at photon energies available for the predefined energies. The software is freely available online after having registered to the Phy-X platform.

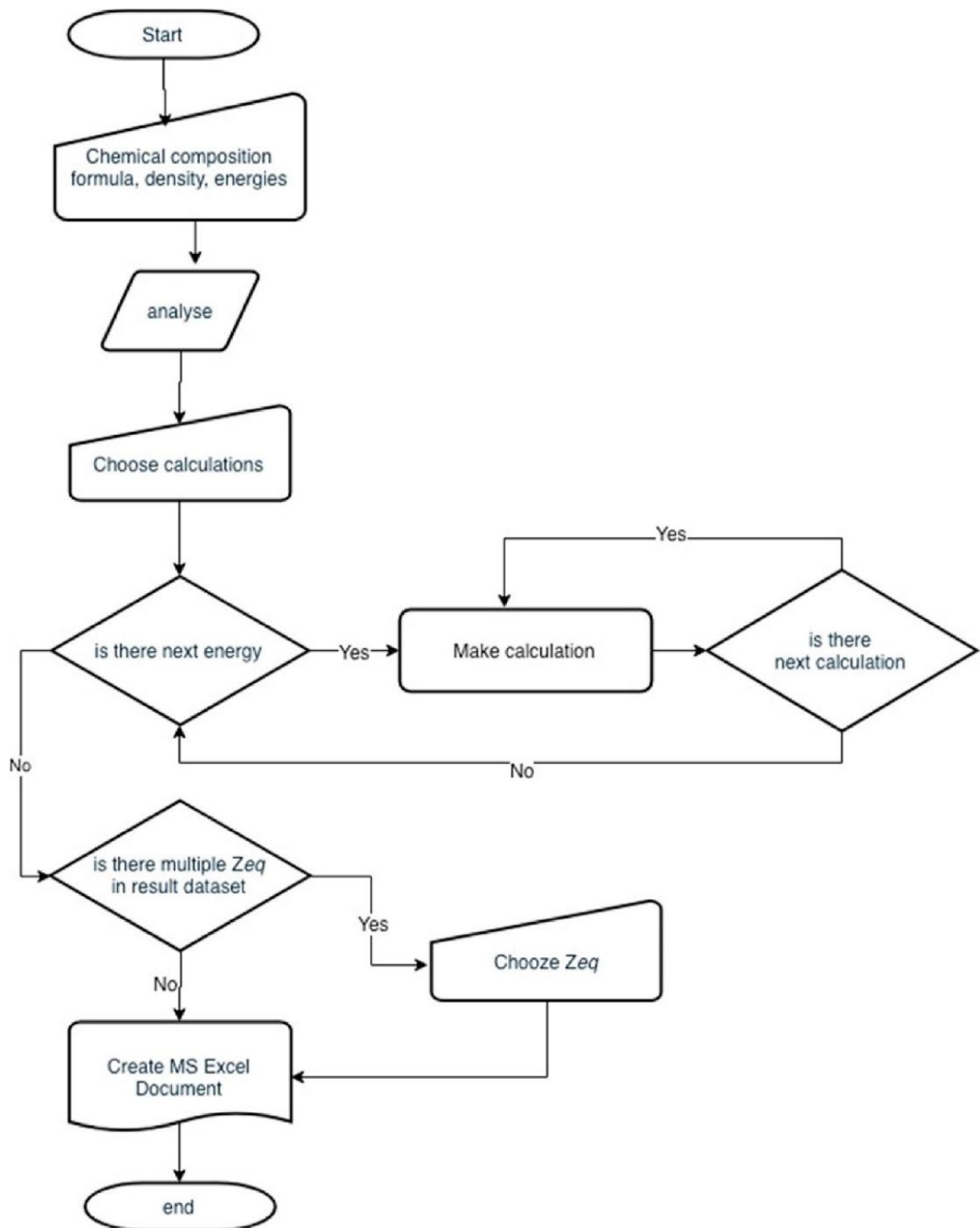


**Figure 0.1:** Flow chart of the PSD online software

This is how the procedures (18), could witness while using this software. The PSD software have been developed which can simultaneously calculate all above mentioned shielding and dosimetry parameters in continuous energy range and at

selected energies in a fast and accurate way for an infinite number of different materials.

### **The Phy-X/PSD online software**

The Phy-X/PSD online software is running on remote server that has Intel(R) Core(TM) i7-2600 CPU @ 3.40 GHz CPU with 1 GB installed memory and operating system is Ubuntu 14.04.3 LTS. The application language is NodeJS v8.4.0 serving with Nginx 1.15.8. Security between client's browser and server is being established with 256 Bit Positive SSL. In order to use the PSD software, the users must have access to the web page of <https://phy-x.net/PSD>. The flow chart and the main screen interface of the PSD online software are shown in Figs. 1 and 2, respectively. Users must register with the Phy-X platform in order to calculate the radiation shielding parameters of any material. The registration process can be completed by verification using only academic-mail addresses. There are three steps which are necessary for calculation in the software and are listed as follows:

The first step is to define the composition of the material to be used in calculations accurately. In the software, the material composition can be entered in two different ways such as mole fraction and weight fraction.

Second step is selection of energies Two energy regions have been predefined in the software as 15 keV-15 MeV (relevant to ANSI database and is used in calculation of EABF and EBF) and 1 keV-100 GeV. Also, some well-known radioactive sources ( $^{22}\text{Na}$ ,  $^{55}\text{Fe}$ ,  $^{60}\text{Co}$ ,  $^{109}\text{Cd}$ ,  $^{131}\text{I}$ ,  $^{133}\text{Ba}$ ,  $^{137}\text{Cs}$ ,  $^{152}\text{Eu}$  and  $^{241}\text{Am}$ ) along with their energies and some characteristic X-ray energies obtained through secondary sources (the K-shell energies of Cu, Rb, Mo, Ag, Ba and Tb elements) are available in the software and can be selected by the user.

Third step is selection of parameters to be calculated, Users can choose which parameter(s) they want to calculate depending on their studies.

After the steps completed successfully, users can save the calculation results in a well-designed MS excel file.

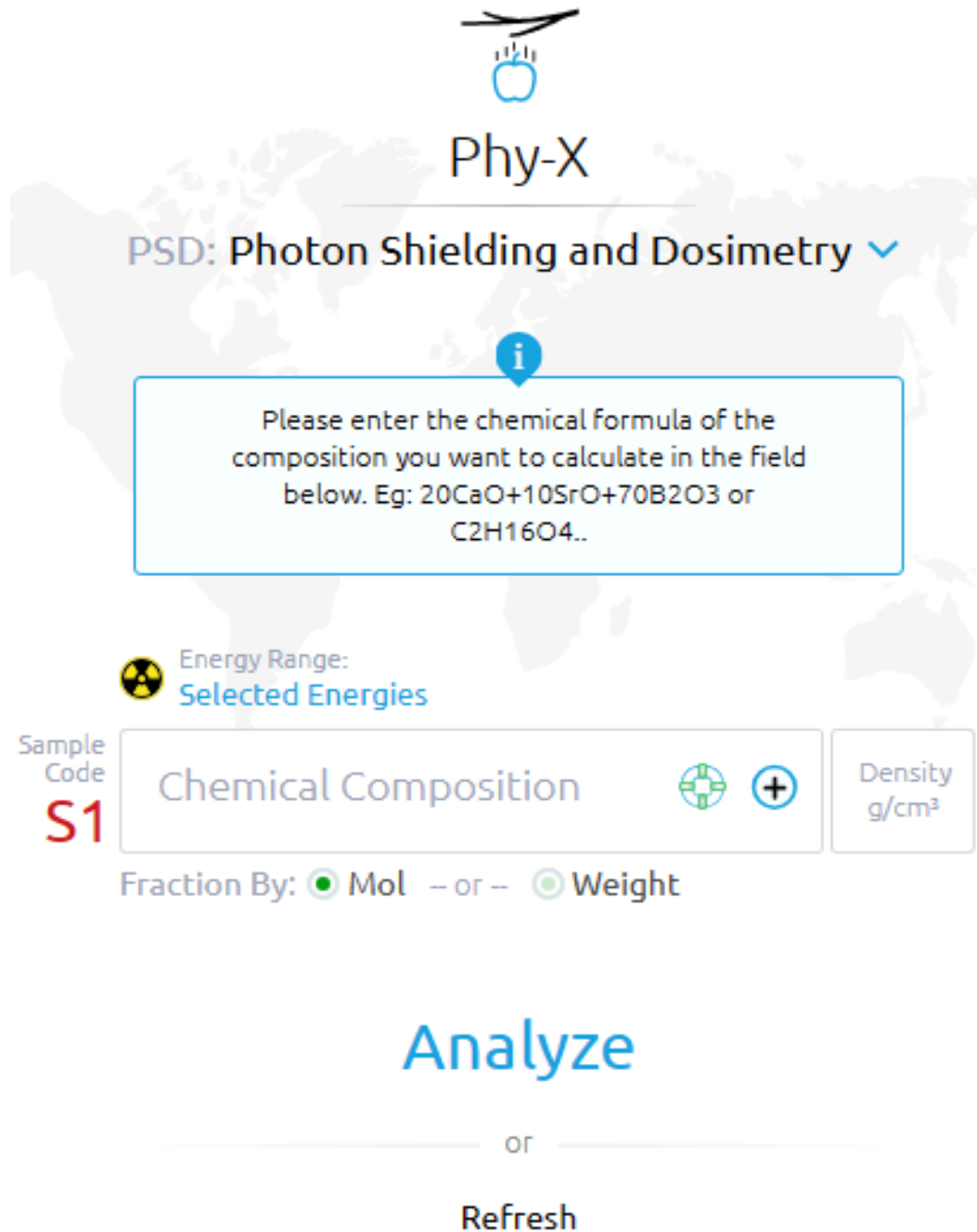


**Figure 0.2:** The main screen interface of the PSD online software

## 2.5 RADIATION SHIELDING PARAMETERS

### Mass attenuation coefficient (MAC)

The MAC value indicates the capacity of ionizing photons passing through the material of a certain thickness. The MAC value of alloy, compound, or mixture systems can be calculated by using the following mathematical equation, where is the MAC value,  $\rho$  is the density value of the material, and with is the fractional weight of the element. The MAC value is one of the most basic calculation methods in radiation

protection studies as it gives the measure of the direct interaction of ionizing radiation with the material [21]. In this point of view, the investigation of MAC value in radiation physics, medical radiation, radiotherapy, and nuclear studies has been used widely. The MAC value is acquired by dividing the LAC value by the density of the glasses. The MAC graph drawn for the glass samples. Obviously, the LAC and MAC function is the same as the tendencies of change. Higher MAC means a higher probability of photon interaction; hence, better attenuation (absorption/scattering). It can be calculated by Beer-Lambert's law as follows;

$$I = I_0 e^{-\mu t} \quad 0.19$$

$$\mu_m = \frac{\mu}{\rho} = \frac{\ln\left(\frac{I_0}{I}\right)}{\rho t} = \frac{\ln\left(\frac{I_0}{I}\right)}{t_m} \quad 0.20$$

where  $I_0$  is the intensity of incident photon and  $I$  is the intensity of attenuated photon beam,  $\mu$  and  $\mu_m$  are linear and mass attenuation coefficients,  $t$  and  $t_m$  are the thickness and mass thickness (mass per unit area) of the material,  $\rho$  is the density of the material.

### **Linear attenuation coefficient (LAC)**

Linear attenuation coefficient measures the decrease in intensity of radiation while passing through a target material. Probability of interaction of radiation per unit length of a given absorber characteristics its LAC value. When a gamma-ray travel thorough a matter, it loses the energy via interaction with the electrons of the matter. Therefore, the higher the density of electrons in a matter, the more probability of interaction and energy loss of gamma-rays. Since the electron density is approximately proportional to the density of the material, the attenuation coefficient depends largely on the density of the material. In short LAC depends on the materials property. Attenuation of gamma rays can be measured according to Beer-Lambert's law:

$$I = I_0 \exp(-\mu t) \quad 0.21$$

$$\mu = \frac{1}{t} \ln\left(\frac{I_0}{I}\right) \quad 0.22$$

where  $I_0$  is the initial photon intensity,  $I$  is the transmitted photon intensity,  $t$  is the penetration depth (cm), and  $\mu$  is the total linear attenuation coefficient at specific photon



energy. The value of LAC can be determined by multiplying the value of MAC with (mass density) if MAC is known.

### **Tenth Value Layer (TVL)**

The Tenth value layer (TVL) is defined as the thickness of a shield or an absorber that reduces the radiation level by a factor of one tenth (10%) of the initial level. It is measured in unit of distance (mm or cm). The amount of radiation that penetrates through a specific thickness of material is determined by the energy of the individual photons and the characteristics (density and atomic number) of the material. It can be calculated by the equation,

$$TVL = \frac{\ln(10)}{\mu} = \frac{2.302}{\mu} \quad 0.23$$

$$Ratios = \left(\frac{\mu}{\rho}\right)_{com} / \left(\frac{\mu}{\rho}\right)_{total} \quad 0.24$$

The ratio in the context of glass radiation shielding signifies the comparison between the mass attenuation coefficient of a specific component within the glass and the mass attenuation coefficient of the entire glass mixture.

$\left(\frac{\mu}{\rho}\right)_{com}$  represents the mass attenuation coefficient for a specific component (e.g., a heavy metal oxide) within the glass. Indicates how effectively that specific component attenuates ionizing radiation (such as X-rays or gamma rays)

$\left(\frac{\mu}{\rho}\right)_{total}$  denotes the mass attenuation coefficient for the entire glass material, considering all its components. Reflects the overall radiation shielding capability of the glass. A higher ratio indicates that the specific component contributes significantly to the overall radiation shielding efficiency of the glass. Designers can optimize glass composition by adjusting the proportion of different components to achieve favorable ratios for specific applications

### **Half Value Layer (HVL)**

Half value layer is the minimum thickness of absorber material at which transmitted radiation intensity becomes half of initial value. It is measured in the unit of distance (cm or mm). The concept of HVL and TVL is very useful in doing rapid, approximate shielding calculations. It is a function of Linear attenuation coefficient.

$$HVL = \frac{\ln(2)}{\mu} \quad 0.25$$

It is a radiation energy dependent parameter, thus the HVL of a material increases with increasing the penetrating photon energy because as energy of incoming radiation increases material needs to be thicker to reduce the radiation to half the initial value. For a particular energy smaller thickness signifies better shielding.

### **Mean Free Path (MFP)**

It is the average distance travelled by the photon between two consecutive interactions. The sample with low MFP at specific photon energy offers high protection against gamma rays while maintaining similar radiation shielding sample thickness. It can be evaluated from linear attenuation coefficient ( $\mu$ ) as per the formula,

$$MFP = \frac{1}{\mu} \quad 0.26$$

### **Effective electron density ( $N_{eff}$ )**

The effective electron number or electron density ( $N_{eff}$ ) can be described as the number of electrons which interacted with photons per unit mass. The value of can be determined from the values of mass attenuation coefficient ( $\mu_m$ ) and total electronic cross section ( $\sigma_e$ ).

$$N_{eff} = \frac{\mu_m}{\sigma_e} \quad 0.27$$

Where the total electronic cross section( $\sigma_e$ ) can be calculated as,

$$\sigma_e = \frac{1}{N_A} \sum_i \frac{f_i A_i}{Z_i} (\mu_m)_i \quad 0.28$$

Where  $f_i$  is the fractional abundance of  $i^{th}$  element and  $Z_i$  is the atomic number of the  $i^{th}$  element.

The effective electron number ( $N_{eff}$ ) can also be estimated using effective atomic number ( $Z_{eff}$ ) as follows:

$$N_{eff} = \frac{N_A}{M} Z_{eff} \sum n_i \quad 0.29$$

Where  $N_A$  Avogadro's number and  $M$  is the atomic mass of glass.

### **Radiation Protection Efficiency (RPE, %)**

The Radiation Protection Efficiency (RPE), expressed as a percentage, serves as a crucial measure of a material's capacity to absorb, and attenuate incoming energetic photons.

$$RPE (\%) = (1 - e^{-LAC \times X}) \times 100 \quad 0.30$$

X is the thickness or depth of the material that the radiation passes through.

### **Effective conductivity**

Effective Conductivity of materials is directly proportional to Neff and density of the material. It is given by following equation,

$$C_{eff} = \frac{N_{eff} \rho e^2 \tau}{m_e} \quad 0.31$$

where e and me are charge and mass of electron, respectively.  $\tau$  is the average life time (relaxation time) of the electron at the Fermi Surface. High value of Ceff indicates that the material can shield radiation more effectively.

### **Equivalent Atomic Number Zeq**

The equivalent atomic number represents the average atomic number of the atoms surrounding a central metal ion in a coordination complex. The equivalent atomic number influences how effectively the glass attenuates ionizing radiation (such as X-rays or gamma rays). Glass compositions with higher equivalent atomic numbers tend to exhibit better radiation attenuation. Heavy metal oxides (with higher atomic numbers) contribute significantly to the overall shielding efficiency of radiation shielding glass. Understanding the equivalent atomic number helps design effective radiation shielding glass by optimizing its composition and properties. , greater equivalent atomic number corresponds to higher radiation shielding efficiency in materials. When the equivalent atomic number is higher, the material tends to be more effective at attenuating ionizing radiation (such as X-rays or gamma rays)

## CHAPTER 3

### RESULT AND DISCUSSION

#### 3.1 PHYSICAL PROPERTIES

Glass properties like density ( $\rho$ ) and refractive index ( $n_d$ ) are sensitive to the structural changes, softening, compactness of the glass structure, variation in the geometry, coordination number, cross-link density, and interstitial space dimension of the medium. The properties are a prevailing tool in exploring the reflection of the structural changes that occurred in the composition. Fluid displacement method. Archimedes principle was used to measure the  $\rho$  values of the prepared glasses which are submitted in Table 1. The determined values show the relationship between masses and volumes, even the  $n_d$  values are in accordance with  $\rho$  values of the specimens. The data displays that  $\rho$  rises with a rise in MgO concentration and reduction in  $B_2O_3$  Content due to the replacement of lighter  $B_2O_3$  atoms (molar mass =69.6182) by heavy MgO atoms (molar mass=40.3044). The molar volume ( $V_m$ ) of the glass samples is the volume occupied by the unit mass of the glass and it is noticed to reduce with a rise in  $\rho$  and  $n_d$  for the equipped glasses (Table 1). The relationship among  $n_d$ , and  $V_m$  is depicted in Fig. 1. The molar refractivity ( $R_m$ ) of the samples is determined by the following relation  $R_m = \left( \frac{n_d^2 - 1}{n_d^2 - 2} \right) V_m$ ,  $n_d$  refractive index of the glass samples.  $R_m$  defines the total polarizability of a mole.

Table 3.1 depicts the determined physical properties of the studied glasses. It is clear from the table that the density ( $\rho$ ) value of the studied glasses increases from 3.64g/cm<sup>3</sup> (for 00BTK glass) to 6.33 g/cm<sup>3</sup> (40BTK glass) as the content of  $B_2O_3$  (molecular weight of 69.6182 g/mol) increases which is due to the structural modification and variation in the coordination number and lattice spacing of the glass structure. Refractive index ( $n_d$ ) is one of the crucial features of glass that designates its optical properties and it is found to rise from 1.553 to 1.625

The elevation in  $\rho$  with a rise in  $B_2O_3$  content is predictable by the formation of new links in the glass configuration. The mentioned result will lead to higher volume contraction via a reduction in bond length and inter-atomic separation between the constituting atoms in the glass structure which were computed with relations from the literature (Aboalatta et al., 2021). The evaluation of inter-atomic

separation like  $r(\text{B-B})$  and  $r(\text{Te-Te})$  reveals that the glass with higher content  $\text{B}_2\text{O}_3$  (40BTK) holds higher compactness compared to other glasses.

The calculated two-photon absorption coefficient ( $\beta$ ) value is lower for the proposed xBTK glasses which denote their applicability in signal processing devices. In conclusion the physical properties radiation shielding glasses should be satisfied by the given composition. Few physical properties has tabulated in below tables.

**Table 3.1:** Composition, corresponding glass code, density ( $\rho$ ), and average molecular weight ( $M_{av}$ ) of Potassium Boro Tellurite glasses

<i>SL. NO</i>	<i>Chemical composition (in wt %)</i>	<i>Glass Codes</i>	<i><math>\rho</math> (g/cm<sup>3</sup>)</i>	<i>M<sub>av</sub> (g/mol)</i>
<i>1</i>	$70\text{B}_2\text{O}_3 + \text{TeO}_2 + 15\text{K}_2\text{O} + 15\text{MgO}$	00BTK	3.64	68.91
<i>2</i>	$60\text{B}_2\text{O}_3 + 10\text{TeO}_2 + 15\text{K}_2\text{O} + 15\text{MgO}$	10BTK	3.96	77.98
<i>3</i>	$50\text{B}_2\text{O}_3 + 20\text{TeO}_2 + 15\text{K}_2\text{O} + 15\text{MgO}$	20BTK	4.82	86.91
<i>4</i>	$40\text{B}_2\text{O}_3 + 30\text{TeO}_2 + 15\text{K}_2\text{O} + 15\text{MgO}$	30BTK	5.13	95.90
<i>5</i>	$30\text{B}_2\text{O}_3 + 40\text{TeO}_2 + 15\text{K}_2\text{O} + 15\text{MgO}$	40BTK	6.33	104.90

## STRUCTURAL PROPERTIES

**Table 3.2:** Structural properties of xBTK glasses

<i>Structural properties</i>	<i>00BTK</i>	<i>10BTK</i>	<i>20BTK</i>	<i>30BTK</i>	<i>40BTK</i>
<i>Metallization criterion, M</i>	0.679	0.670	0.662	0.651	0.646
<i>Tellurium Tellurium separation d(Te Te)</i>	3.57	3.42	3.15	3.03	2.77
<i>Optical bandgap E<sub>g</sub></i>	4.082	4.043	4.020	3.985	3.966
<i>Two Photon absorption coefficient <math>\beta</math> (cm/GW)</i>	3.593	3.868	4.020	4.377	4.534
<i>Distribution density of Te, Dd(B)</i>	1.89	1.74	1.75	1.62	1.67
<i>Optical basicity (<math>\Delta\theta</math>)</i>	0.617	0.646	0.666	0.691	0.714
<i>Molar polarizability (<math>\alpha_m</math>)</i>	2.404	2.578	2.417	2.582	2.324
<i>Oxygen molar Volume</i>	8.167	8.842	8.506	9.384	9.008
<i>Refraction loss (R%)</i>	4.691	4.972	5.202	5.503	5.668
<i>Optical electronegativity <math>\chi_{opt}</math></i>	2.073	2.030	1.996	1.953	1.929
<i>Dielectric Constant <math>\epsilon</math></i>	2.411	2.477	2.531	2.601	2.640

### **Tellurium -Tellurium distance $r(\text{Te-Te})$ and density distribution of Tellurium $D_{d(\text{Te})}$ :**

Structural features like boron-boron separation  $r(B-B)$ , and tellurium-tellurium separation  $r(\text{Te-Te})$  aid in examining the compactness of the glass structure. Tellurium atoms are the fundamental components in glass; therefore, the separation between these atoms can indicate the compactness of the glass structure. From TABLE 3.2, it is observed that the value of  $r(\text{Te-Te})$  is high for 00BTK glass (3.57 Å) while it is low for 40BTKglass (2.77 Å). This decrease in  $r(\text{Te-Te})$  can be attributed to the decrease in the molar fraction of boron atoms as we move from 00BTK to 40BTK samples. The decrease in the average tellurium-tellurium separation indicates a closer packaging of the glass structures, particularly noticeable in the 40BTK sample. Furthermore, from Table 2, it is evident that the value of Distribution density of tellurium,  $D_{d(\text{Te})}$  is high for 00BTK glass, with a value  $1.89 \times 10^{-13} \text{ m}^{-2} \text{ mol}^{-1}$ , while it is low for 40BTK glass, which has a value  $1.67 \times 10^{-13} \text{ m}^{-2} \text{ mol}^{-1}$ .

### **Oxygen Packing Density (OPD) and Molar Volume of Oxygen ( $V_o$ ):**

The oxygen packing density in glass refers to how closely oxygen atoms are packed in the glass structure. The oxygen packing density in glass is a critical parameter that affects a wide range of properties, including structural integrity, chemical and thermal stability, optical performance, and manufacturing characteristics.

The molar volume of oxygen in the context of glass refers to the amount of space occupied by one mole of oxygen gas. The molar volume of oxygen, when considering its presence in glass compositions, contributes to the overall density and structure of the glass. It plays a role in determining how closely atoms and molecules are packed within the glass matrix. The arrangement of oxygen atoms is a fundamental aspect of the glass structure, influencing properties such as density and strength. The molar volume of oxygen in glass is a crucial parameter that affects various aspects of glass properties, including structure, density, thermal expansion, chemical stability, and manufacturing processes.

The Oxygen packing density (OPD) and molar volume of oxygen ( $V_o$ ) explain the packing density of oxygen atoms within the glasses. Throughout the series of glasses, the molar volume of oxygen ( $V_o$ ) and OPD values exhibit contrasting trends, with  $V_o$  increasing while OPD decreases. The molar volume of oxygen correlates with

the total molar volume of the glass. The decrease in OPD content is directly associated with a reduction in the number of oxygen atoms. . From Table 2, the highest OPD value, indicating a tighter structure, is observed for 00BTK glass at 126.773 mol/cm<sup>3</sup>, thus this glass has more bridging oxygens, and the lowest value of OPD is 112.33 mol/cm<sup>3</sup> for 30BTK glass.

#### **Metallization Criterion (M) and Optical Band gap energy (E<sub>g</sub>):**

The metallization criterion (M) was explored to determine the metallic or non-metallic character of the fabricated glasses. M values less than 1 indicate the non-metallic or insulating character of the produced glass systems. From TABLE 2, all samples had M values varying between 0.6799 and 0.64646.

The optical band gap energy of a material, including glass, refers to the energy difference between the highest energy (valence) band of electrons and the lowest energy (conduction) band where electrons are free to move and conduct electricity. In the context of glass, the optical band gap is primarily associated with the electronic transitions that occur when photons with energy corresponding to the band gap are absorbed. The optical band gap energy in glass plays a crucial role in determining its optical and electronic properties. It affects the material's transparency, color, and its ability to absorb or transmit light in different regions of the electromagnetic spectrum. The band gap energy can be influenced by the composition and structure of the glass. , M values were derived using the refractive index (n<sub>d</sub>) and the energy band gap (E<sub>g</sub>). M is calculated to demonstrate the non-metallic nature of the samples, and it is observed to decrease with a reduction in the optical band gap (E<sub>g</sub>), which is calculated from n<sub>d</sub> and falls in the range of 1.553-1.625eV for the xBTK glasses. Both M and E<sub>g</sub> decrease with an increase in n<sub>d</sub> for all the samples.

#### **Two-photon absorption (β) and Optical Basicity (Λ<sub>th</sub>)**

Glasses that exhibit nonlinear optical properties hold significant promise for photonic applications. Two-photon absorption (β) occurs when two photons of the same or different energies are absorbed. β values were computed for the xBTK glass set, and higher values of β lead to promising applications in power limiters, real-time holography, ultrafast optical switches, self-focusing, and white light continuum generation. Band gap values are utilized in calculating the β values as presented in Table 3.2 The values range from 3.597 to 4.53435 (cm/GW) for 00BTK-40BTK glasses, respectively.

Optical basicity is not a direct method to calculate the actual basicity of the glass. It is theoretically calculated using the individual basicity of the oxides taken for synthesizing glass. From Table 3.2, the  $\Lambda$ th value is higher for 40BTK glass, rising from 0.671 to 0.714, which is due to the increase in the number of non-bridging oxygen atoms in the glass matrix.

#### **Molar Polarizability ( $\alpha_m$ ) :**

Molar polarizability is a measure of the ability of an atom or a molecule to undergo polarization in the presence of an electric field. In the context of radiation shielding glass, the molar polarizability of the glass material can play a role in its effectiveness as a radiation shield. The molar polarizability, along with other material properties, can influence the structural integrity of the glass. Higher molar polarizability may lead to increased interaction with radiation, potentially enhancing the shielding capability of the glass. . It affects various characteristics such as refractive index. From the TABLE 2, the molar polarizability ( $\alpha_m$ ) of the prepared glass samples vary from 2.40 to 2.58 for 00BTK to 30BTK, respectively. The sample 30BTK has the highest molar polarizability.

#### **Reflection Losses (R%)**

Refraction loss refers to the reduction in the intensity of reflected or refracted light as it interacts with a surface, refraction loss occurs when light waves pass from one medium to another, leading to a reduction in intensity due to absorption or other factors. It's a fascinating phenomenon that shapes our understanding of light behavior. They can impact the optical properties of glass samples and reduce the effectiveness of the shielding material by allowing some radiation to penetrate the material. A glass sample with low reflection losses is essential to maximize the transparency and effectiveness in blocking or attenuating radiation. From TABLE 2, the reflection losses varies from 4.46919 (00BTK) to 5.6689 (40BTK), with the glass sample 00BTK exhibiting the minimum reflection losses.

#### **The dielectric constant, $\epsilon$**

The dielectric constant, also known as the relative permittivity, measures how well a material can store electrical energy in an electric field. It quantifies the ability of a material to polarize when subjected to an electric field. A higher dielectric constant can lead to a wider band gap, affecting the glass's transparency to different wavelengths of light. Glasses with specific dielectric constants may absorb or transmit



certain wavelengths more effectively. Radiation shielding glass with a higher dielectric constant can effectively absorb ionizing radiation (such as gamma rays and X-rays). The dielectric constant varies from 2.411809 to 2.640625 for 00BTK to 40BTK, higher value of dielectric constant is for 40BTK, therefore this composition has higher radiation shielding efficiency.

### Optical electronegativity

The optical electronegativity of glass plays a significant role in determining its radiation shielding properties. The optical electronegativity is a measure of how strongly an atom attracts electrons in the context of optical properties. It influences the behavior of light when it interacts with the glass material. The optical electronegativity affects the glass's ability to absorb radiation.

Higher electronegativity tends to enhance absorption due to stronger interactions between electrons and incident radiation.

Higher optical electronegativity is for 00BTK is 2.073799 and optical electronegativity decreases on increasing the TeO<sub>2</sub>, hence low optical electronegativity for 40BTK glass 1.929734, hence its efficiency decreases in shielding, due to decrease in absorption and scattering radiation.

### Ionic ( $I_C$ %) and Covalent character ( $C_C$ %)

**Table 3.3:** Ionic character factor ( $I_C$ %) and covalent factor ( $C_C$ %) of Potassium Boro Tellurite glasses

<i>Chemical Compound</i>	<i>Electronegativity of elements</i>	$XC$	$XA$	$\Delta X$	$I_C(\%)$	$C_C(\%)$
<b>B<sub>2</sub>O<sub>3</sub></b>	B(2.04), O(3.44)	4.08	10.32	6.24	99.9941	0.00592
<b>TeO<sub>2</sub></b>	Te(2.1)	2.1	6.88	4.78	99.6694	0.33057
<b>K<sub>2</sub>O</b>	K(0.82)	1.64	3.44	1.8	55.5142	44.4858
<b>MgO</b>	Mg(1.31)	1.31	3.44	2.13	67.8329	32.1671

<i>Glass code</i>	<i>Composition</i>	$I_C(\%)$	$C_C(\%)$
<b>00BTK</b>	70B <sub>2</sub> O <sub>3</sub> +TeO <sub>2</sub> +15K <sub>2</sub> O+15MgO	89.4946	11.5054
<b>10BTK</b>	60B <sub>2</sub> O <sub>3</sub> +10TeO <sub>2</sub> +15K <sub>2</sub> O+15MgO	88.4654	11.5346
<b>20BTK</b>	50B <sub>2</sub> O <sub>3</sub> +20TeO <sub>2</sub> +15K <sub>2</sub> O+15MgO	88.433	11.567
<b>30BTK</b>	40B <sub>2</sub> O <sub>3</sub> +30TeO <sub>2</sub> +15K <sub>2</sub> O+15MgO	88.4005	11.5995
<b>40BTK</b>	30B <sub>2</sub> O <sub>3</sub> +40TeO <sub>2</sub> +15K <sub>2</sub> O+15MgO	88.3681	11.6319

The choice between ionic and covalent bonding in the composition of radiation shielding glass can have significant implications for its properties and effectiveness. Both types of bonding contribute to the overall characteristics of the material, influencing factors such as density, transparency, and attenuation of radiation. Both ionic and covalent bonding play important roles in the design and performance of radiation shielding glass. Ionic bonding occurs when electrons are transferred from one atom to another, resulting in the formation of positively and negatively charged ions. Excessive ionic character can lead to lower chemical durability and increased susceptibility to environmental degradation. " $I_C$ " denotes the ionic factor.

Covalent bonding involves the sharing of electron pairs between atoms, resulting in the formation of strong chemical bonds. The presence of covalent bonds can enhance the glass's ability to attenuate ionizing radiation by absorbing and scattering radiation particles. " $C_C$ " denotes the covalent factor  $\Delta\chi$  (Pauli electronegativity) represents the electronegative difference ( $\Delta\chi = X_C - X_a$ ) between the anions ( $X_a$ ) and cations ( $X_c$ ) of the glass matrix. . From Table 3.3, the present glasses show decreased ionicity ( $I_C > 99\%$ ) from the glass sample 00BTK to 40BTK and an increase in covalency ( $C_C > 0.005\%$ ) from 00BTK to 40BTK.

### 3.2 STRUCTURAL CHARACTERIZATION

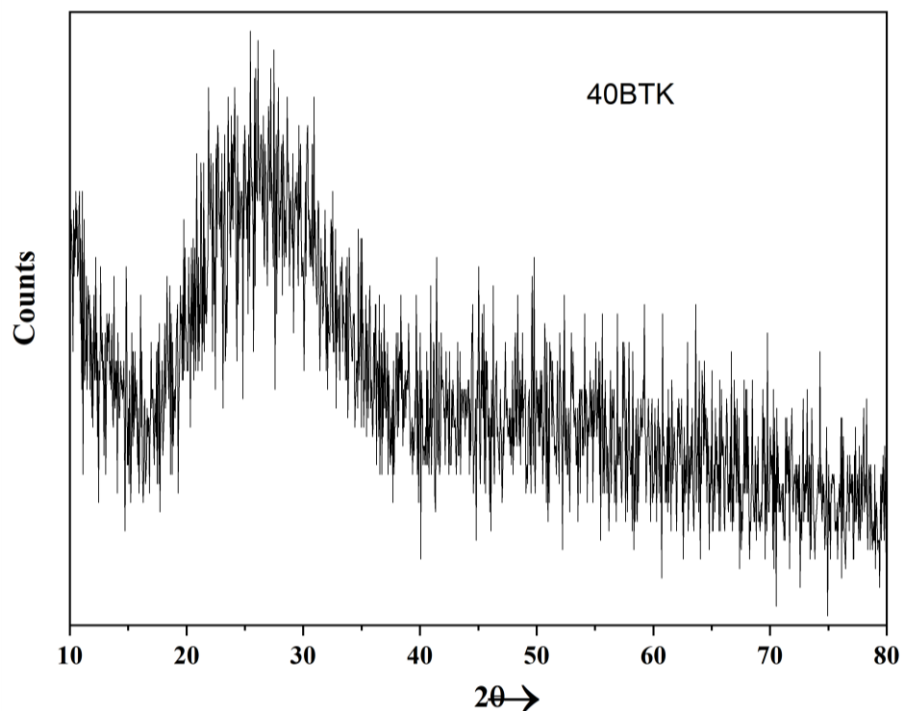


**Figure 3.1.** X-ray Diffraction pattern of 40BTK

The XRD profile of the 40BTK glass sample is shown in Fig 3.1 No specific peaks were observed in the pattern to indicate the crystalline nature. There was no continuous sharp peak observed, demonstrating a typical totally amorphous glass structure without any sign of crystallization. This indicates the lack of long-range atomic order and the presence of short-range atomic order in the glass samples. This provides enough evidence for the amorphous character of the prepared glasses.

### 3.3 RADIATION SHIELDING PROPERTIES

#### 3.3.1 Tenth Value Layer (TVL):

In the context of the investigated glasses, the tenth value layer (TVL) has been determined and is depicted in Fig 3.2, corresponding to photon energies of 3 and 4 MeV respectively.

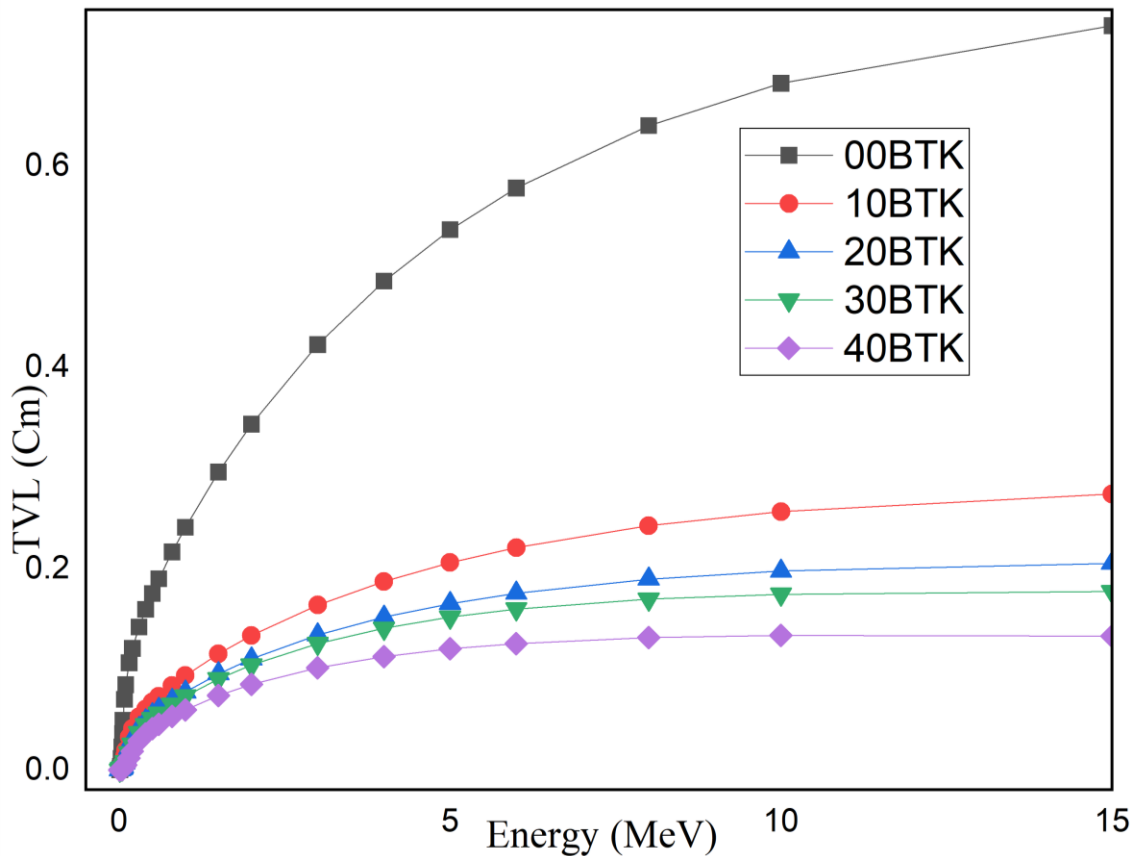


**Figure 0.2** TVL of 00BTK, 10BTK, 20BTK, 30BTK, 40BTK

It is important to keep in mind that the TVL is the thickness of the medium required to bring the photon intensity down to a tenth of its starting value. The lower TVL value indicates better shielding ability. According to Fig the TVL for glasses increases with increasing energy. Thus, it is evident that Fig 3.3.1 TVL values are

different two block graphs, the value on second are significantly higher than first one. This observation is reasoning as higher energy radiation has greater penetration capabilities. For this reason, photons with energy can travel a greater distance before their intensity drops to a sensible level. On comparing the TVL values at two different energy levels such as 0.15MeV and 8MeV the values varies as 00BTK from 0.106609cm to 0.640021, similarly for 40BTK 0.012036 to 0.13148. One can clearly see how density affects radiation shielding when comparing the TVL values for the prepared glasses at two different energies. TVL values are higher in glass with lower density and vice versa.

### 3.3.2 Mean Free Path (MFP)

The MFP can be used to elucidate the relative photon shielding ability of a medium with respect to others. It is the mean path length of a photon travels between two successive interactions leading to energy loss or absorption. Therefore, lower MFP implies more photon interactions and absorption and vice versa.

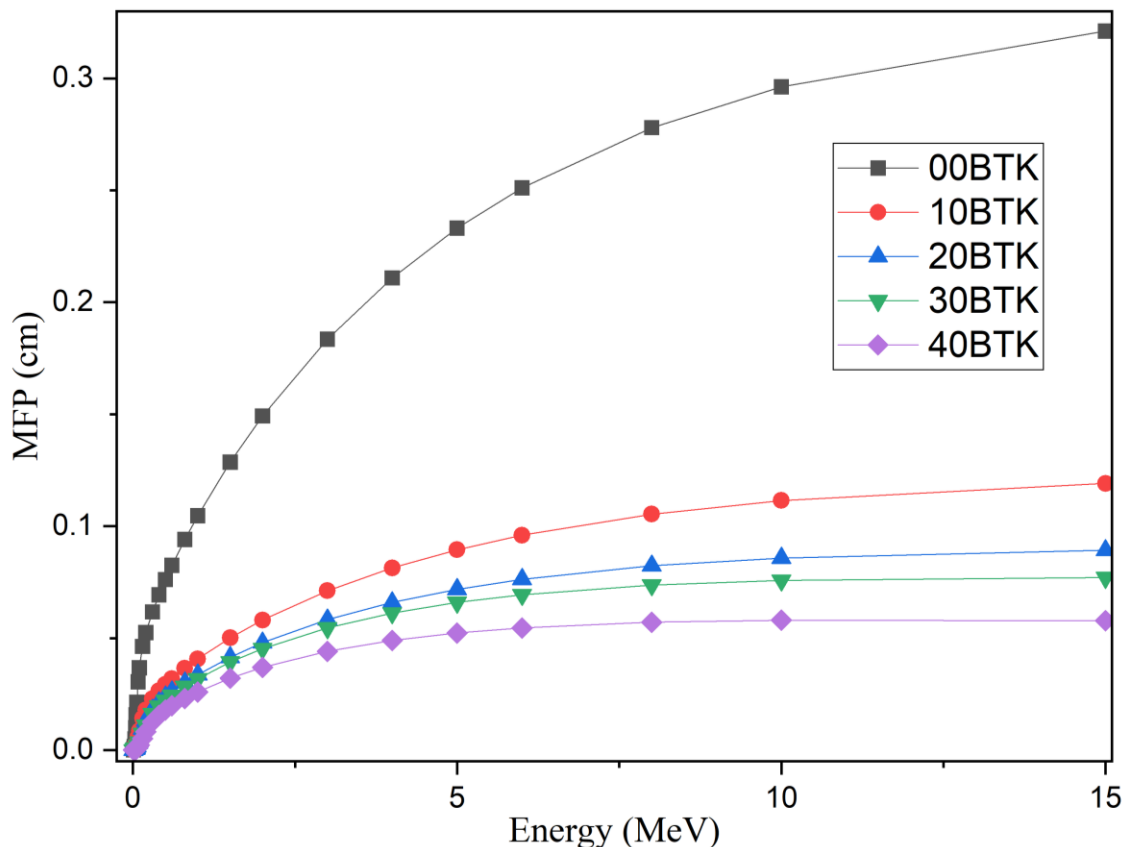


**Figure 0.3** Variation of MFP v/s Gamma Energy

The data of the mean free path (MFP) were used to estimate the effect of TeO<sub>2</sub> on the radiation protection capabilities of the investigated glasses. Designers of

shielding materials and glasses often incorporate heavy metal oxides (HMOs) to minimize the MFP, thereby enhancing radiation protection. In Fig 3.3.2 the MFP findings for the 00BTK to 40BTK samples, as evaluated by PHY-X. High-energy photons may easily pass through 00BTK to 40BTK samples, as shown by the MFP curves, and this is because the MFP rises as photon energy rises. The smallest MFP, which ranged from 0.030475cm (for 00BTK) to 0.001344cm (for 40BTK), was seen at 0.08 MeV. For 00BTK to 40BTK samples, the MFP is determined to be 0.27795, 0.105380, 0.08233, 0.07375 and 0.05710 cm, respectively, at 8MeV. According to Fig3.3.2, the MFP drops as TeO<sub>2</sub> is added, and 40BTK has the lowest MFP while 00BTK has the highest MFP. For the 00BTK and 40BTK samples, the effect of TeO<sub>2</sub> is compared on the MFP at various energy levels.

### 3.3.3 Half Value Layer (HVL)

The half value layer (HVL) of a material is its thickness required to attenuate half of the incoming radiation. HVL is inversely proportional to LAC, which means that a lower HVL signifies a better shield. Additionally, for space constraints, a material that can attenuate the same amount of radiation while occupying less space is more desirable. The HVL of the proposed glass samples was graphed against the photon energy in Fig 3.3.

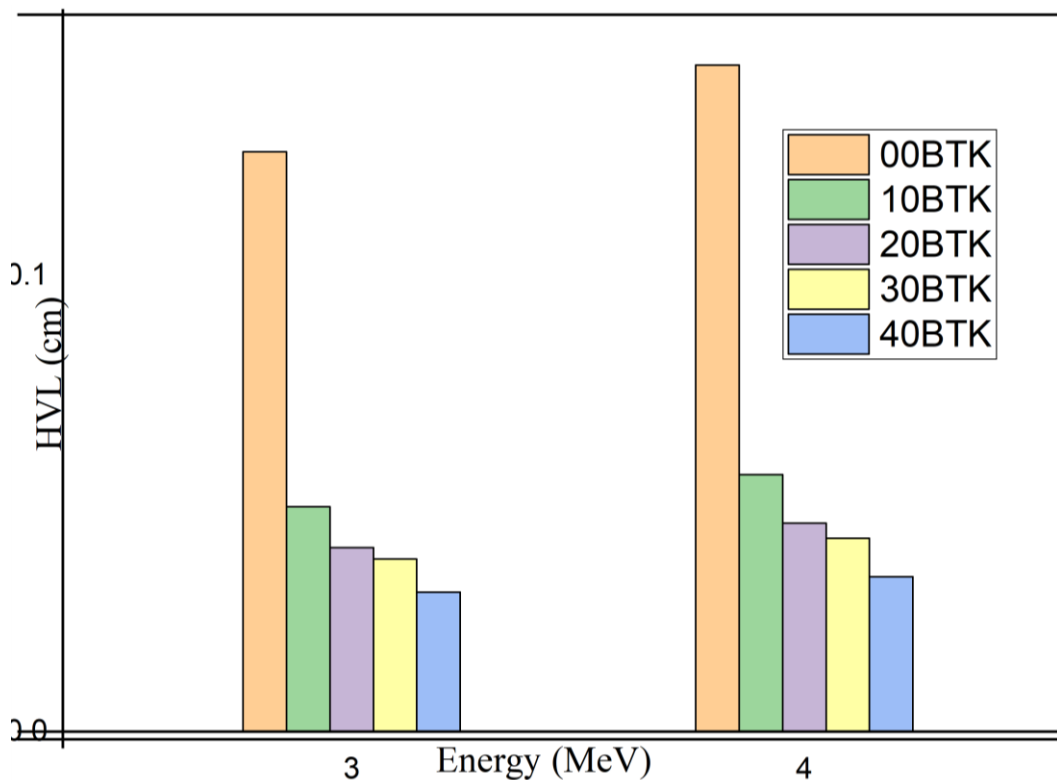


**Figure 1.4** Half Value Layer of glasses at 3 and 4 MeV

As the incoming photon energy increased, the HVL values of all the glasses increased with it. HVL of 40BTK glass on comparing at two different energy levels it shows a difference that is on increasing MeV there is an increase in HVL values too for eg when we compare at 1.5 MeV and 4 MeV it is increased from 0.08911 cm at 1.5 MeV, to 0.14617 cm at 4 MeV, in 00BTK similarly in other cases too. This upward trend occurs because as the incoming photon energy increases, the photons can penetrate through the glasses with greater ease. Therefore, to attenuate the same amount of radiation, the thickness of the glass must increase, thereby increasing HVL. At all energies, however, 40BTK has the least HVL, followed by 30BTK, 20BTK, 10BTK and 00BTK. The HVL values of the glasses at 1.5MeV are equal to 0.08911 cm, 0.034736 cm, 0.02877 cm, 0.02725 cm, and 0.0222760 cm for 00BTK, 10BTK, 20BTK, 30BTK, 40BTK respectively, while at 4.00 MeV, they are equal to 0.14617cm, 0.05640 cm, 0.04573cm, 0.04242 cm and 0.03394cm respectively. These values illustrate the superiority of 40BTK as a radiation shield over the other glasses, as well as highlighting its advantage at higher energies. At low energies, the HVL values of the glasses are extremely close together, but as energy increases, superior radiation shielding of 40BTK can clearly be seen, especially when compared to the lesser shielding capability of 00BTK.

### 3.3.4 Ratios $\left(\frac{\mu}{\rho}\right)_{com}/\left(\frac{\mu}{\rho}\right)_{total}$

The ratio in the context of glass radiation shielding signifies the comparison between the mass attenuation coefficient of a specific component within the glass and the mass attenuation coefficient of the entire glass mixture

$\left(\frac{\mu}{\rho}\right)_{com}$  represents the mass attenuation coefficient for a specific component (e.g., a heavy metal oxide) within the glass. Indicates how effectively that specific component attenuates ionizing radiation (such as X-rays or gamma rays)

$\left(\frac{\mu}{\rho}\right)_{total}$  denotes the mass attenuation coefficient for the entire glass material, considering all its components

Reflects the overall radiation shielding capability of the glass. A higher ratio indicates that the specific component contributes significantly to the overall radiation shielding efficiency of the glass. Designers can optimize glass composition by adjusting the proportion of different components to achieve favorable ratios for

specific applications. On comparing two energy levels lower density composition has higher ratio at lower energy that is at 0.6MeV 00BTK 0.9984633 and at 2MeV at 0.98686, similarly for 40BTK its 0.951845 at 0.6MeV and 0.96248247 at 2MeV. Hence 00BTK has good shielding efficiency.

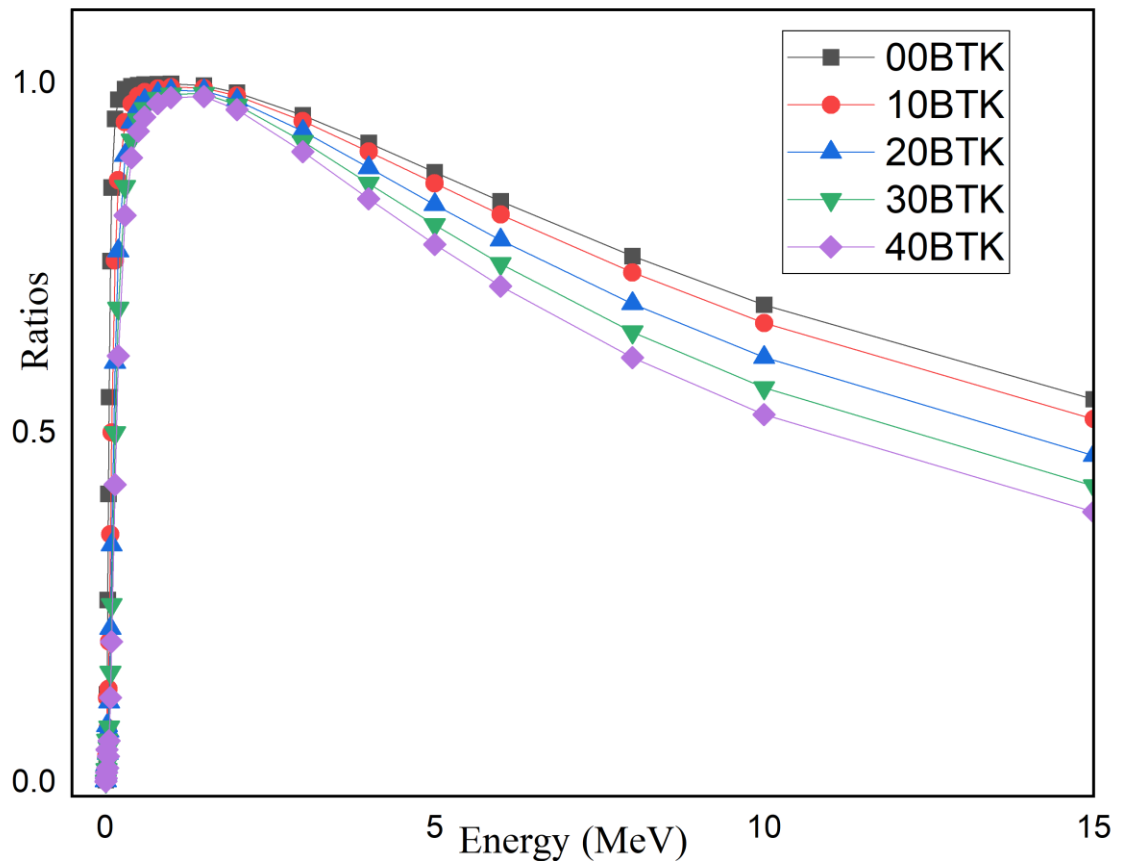
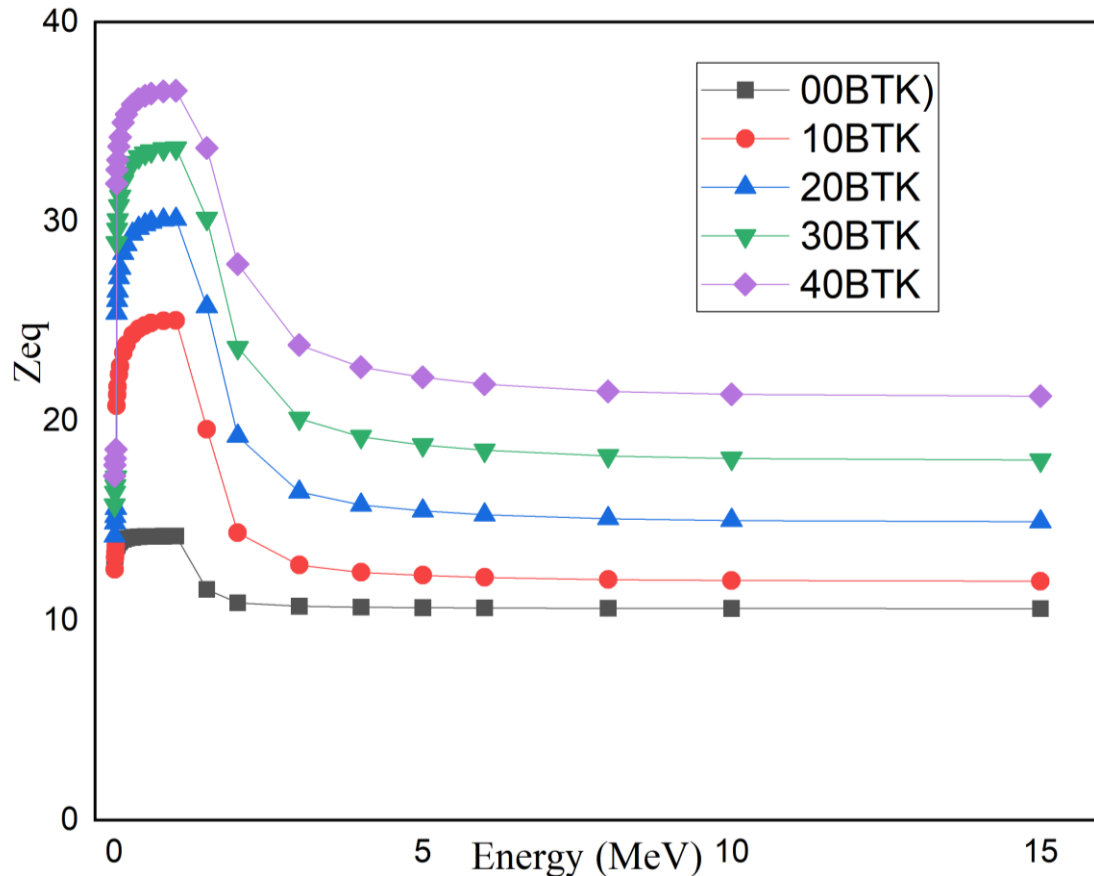


Figure 0.5 Ratios V/S Gamma energy

### 3.3.5 Equivalent Atomic Number $Z_{eq}$

The equivalent atomic number represents the average atomic number of the atoms surrounding a central metal ion in a coordination complex. The equivalent atomic number influences how effectively the glass attenuates ionizing radiation (such as X-rays or gamma rays). Glass compositions with higher equivalent atomic numbers tend to exhibit better radiation attenuation. Heavy metal oxides (with higher atomic numbers) contribute significantly to the overall shielding efficiency of radiation shielding glass. Understanding the equivalent atomic number helps design effective radiation shielding glass by optimizing its composition and properties. , greater equivalent atomic number corresponds to higher radiation shielding efficiency in materials. When the equivalent atomic number is higher, the material tends to be more effective at attenuating ionizing radiation (such as X-rays or gamma rays). However,

other factors (such as density, composition, and thickness) also play a role in determining overall shielding effectiveness. Now considering two different energies could see which one is showing higher efficiency, at 0.5 MeV the  $Z_{eq}$  varies as 14.21657, 24.7986, 29.8514, 33.4249135 and 36.30806 for 00BTK, 10BTK, 20BTK, 30BTK, 40BTK and the  $Z_{eq}$  varies as 10.5966, 11.9715, 14.9568, 18.04445, 21.2459 respectively. Hence higher density composition at lower energy shows greater radiation shielding efficiency.



**Figure 0.6**  $Z_{eq}$  V/S Gamma energy

### 3.3.6 Mass Attenuation Coefficient (MAC)

Theoretical values of the mass attenuation coefficient (MAC) for a selection of glasses, namely 00BTK, 10BTK, 20BTK, 30BTK, and 40BTK, have been investigated and presented in Figure.3.3.6.. These values were determined through calculations using the Phy-X program across the energy range of 0.015 to 15 MeV. The variation in MAC with the energy for the previously mentioned glasses was found to be identical. The trend indicates a decline in MAC values as photon energy increases.



Three fundamental principles governing photon interactions with the glass - namely, photoelectric interaction (PE), Compton scattering (CS), and pair production (PP) are deeply intertwined with the observed behavior of MAC with energy. The maximum MAC is reportedly found at 0.08 MeV (ranging from 9.01456 to 117.522 cm<sup>2</sup>/g), and after that, MAC significantly decreases up to 0.5 MeV. When the energy goes from 0.08 to 0.5 MeV, the MAC drops from 9.01456 to 3.6065 cm<sup>2</sup>/g for 00BTK and from 117.522 to 8.83539 cm<sup>2</sup>/g for 40BTK.

In the low  $\gamma$ -spectrum energy,  $E_\gamma$  region (i.e., PE interaction interval), the  $\mu_m$  values suffer a high reduction, where the  $\mu_m$  values decreased from 9.01456 to 5.933589 cm<sup>2</sup>/g (for 00BTK), from 43.28709 to 17.7986 cm<sup>2</sup>/g (for 10BTK), from 68.0320 to 21.9391403 cm<sup>2</sup>/g (for 20BTK), from 92.77705 to 26.074623 cm<sup>2</sup>/g (for 30BTK), and 117.52203 to 30.26601 cm<sup>2</sup>/g (for 40BTK), respectively, when the  $E_\gamma$  raised from 0.08 to 0.15 MeV. This reduction is primarily attributed to the PE cross-section, with the high atomic number of Tellurite (Te) in the glasses enhancing the probability of PE occurring. Moreover, it is noteworthy that all the selected glasses exhibit approximately the same MAC values between 0.08 and 0.15 MeV, suggesting minimal influence of sample composition on the attenuation trend within this energy range.

The second  $E_\gamma$  interval ranged between 0.15 and 0.3 MeV, a moderate lowering in the  $\mu_m$  values was observed due to the CS interaction cross-section. Compton scattering (CS), which is crucial for these energies, is mostly responsible for this pattern in MAC. As is well known, the likelihood of CS is almost independent of the shielding materials' atomic number (Z). In this interval, the  $\mu_m$  values of the fabricated glass samples decreased from 5.9335 to 4.45188 cm<sup>2</sup>/g (for 00BTK), from 17.7986 to 11.036567 cm<sup>2</sup>/g (for 10BTK), from 26.0746 to 11.5494 cm<sup>2</sup>/g (for 20BTK), from 26.074623 to 12.0622 cm<sup>2</sup>/g (for 30BTK), and from 30.2261 to 12.57508 cm<sup>2</sup>/g (for 40BTK).

In the last region extended from 0.3 to 0.5 MeV, the  $\mu_m$  values lowered slightly under the effect of the PP cross-section. The  $\mu_m$  values decreased from 4.45188 to 3.6065 cm<sup>2</sup>/g (for 00BTK), from 11.036567 to 8.6300 cm<sup>2</sup>/g (for 10BTK), from 11.5494 to 8.6985 cm<sup>2</sup>/g (for 20BTK), from 12.06224 to 8.76696 cm<sup>2</sup>/g (for 30BTK), and from 12.5750899 to 8.83539 cm<sup>2</sup>/g (for 40BTK).

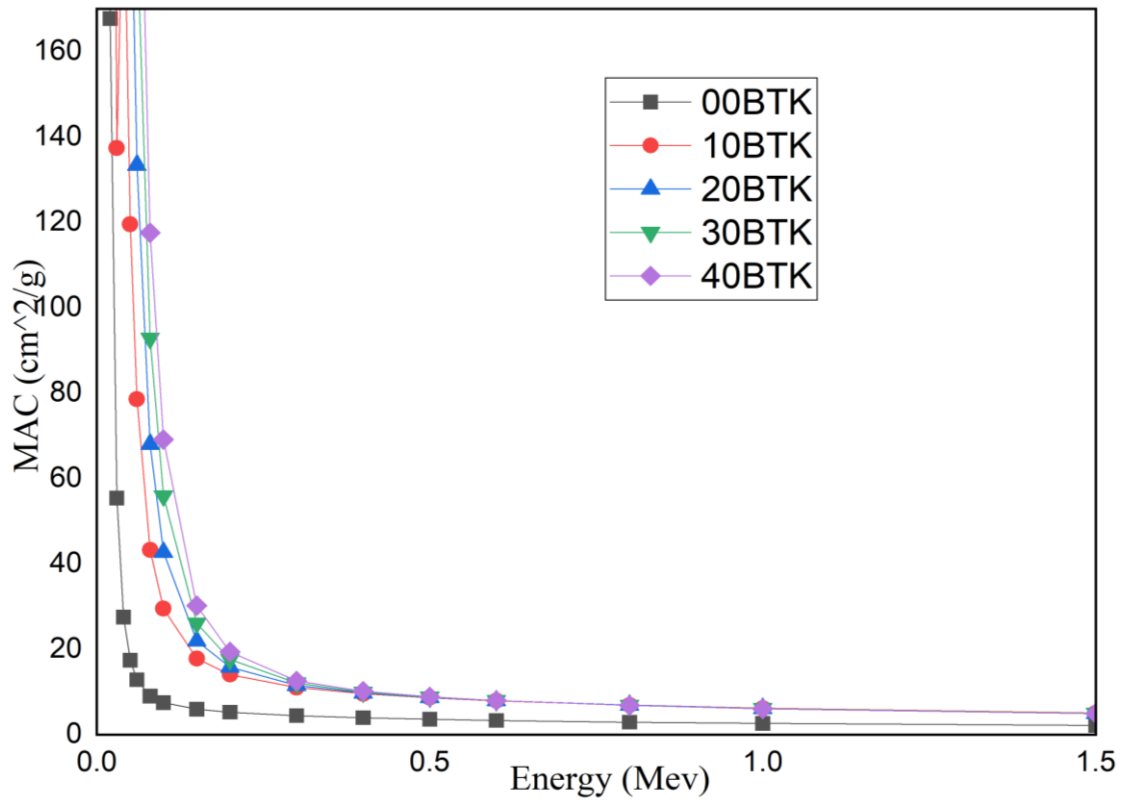


**Figure 0.7** MAC V/S Gamma Energy variations

## CHAPTER 4

### CONCLUSION

This study evaluated the radiation shielding ability of Potassium Boro Tellurite glass systems having the composition  $70\text{B}_2\text{O}_3+x\text{TeO}_2+15\text{K}_2\text{O}+15\text{MgO}$  with  $x=0,10,20,30$  and  $40$  wt%. The glasses were meticulously prepared using traditional melt-quenching technique. Structural features such as tellurium-tellurium distance, density distribution, metallization criterion, and optical band gap were computed, indicating modifications in the glass structure. Different radiation shielding parameters like MAC, HVL, TVL, MFP,  $Z_{\text{eq}}$  etc were calculated using Phy-X software. Physical attributes such as density, refractive index, average molecular mass, molar volume, and molar refractivity were determined, with the 40BTK glass demonstrating higher density and refractive index. MAC results showed an increment with increase in concentration of  $\text{TeO}_2$ , thus 40BTK showed the highest MAC value owing to the highest amount of  $\text{TeO}_2$ . An upward trend was observed in HVL and TVL values with increase in energy of radiation. As concentration of  $\text{TeO}_2$  increased, HVL and TVL values decreased. The least value for both HVL and TVL was exhibited by most dense sample 40BTK and the highest HVL and TVL value by the least dense sample 00BTK. On increasing the concentration of  $\text{TeO}_2$ , 40BTK exhibit the lowest value for MFP (Mean Free Path). In case of  $Z_{\text{eq}}$ , on increasing concentration of  $\text{TeO}_2$   $Z_{\text{eq}}$  value increases that is highest value is exhibited by 40BTK. Similarly other three structural parameters are also explained. The structural properties like Tellurium-Tellurium distance, Dielectric constant, Metallization criteria, Optical band gap, Two photon absorption coefficient, Reflection loss, Oxygen Packing Density, Optical basicity, Optical electronegativity etc were computed and 40BTK show the tighter structure. Thus, it can be concluded that the sample with highest density 40BTK is a better shield and among the glass samples under consideration as the concentration of  $\text{TeO}_2$  increased its radiation shielding performance got better.

## **CHAPTER 5**

### **FUTURE PROSPECTS AND PRESENTATION**

#### **5.1 FUTURE SCOPE**

**Radiation Shielding:** This radiation shielding glasses offer effective protection against ionizing radiation, making them crucial for nuclear facilities, medical applications, and space exploration.

**Optical Transparency:** Their transparency allows for visibility and control of experimental conditions, making them valuable in environments where visibility is essential.

**Mechanical Resilience:** Structural glasses provide robustness and durability, ensuring reliable performance in demanding conditions such as aerospace or industrial settings.

**Material Innovation:** Ongoing research aims to enhance the shielding capabilities of these glasses through innovative material formulations and processing techniques.

**Nanomaterials:** Integration of nanoparticles into glass matrices could lead to enhanced radiation attenuation properties and novel functionalities.

**Cost-Effectiveness:** Development efforts target cost-effective manufacturing processes to make these glasses more accessible for widespread use across industries.

**Biomedical Applications:** The biocompatibility of certain glass compositions opens up possibilities for medical applications such as implants and drug delivery systems.

**Environmental Remediation:** Glasses with heavy metal oxides can immobilize pollutants, offering potential solutions for environmental cleanup efforts.

**Energy Storage:** Zinc doped glasses have been explored for their potential in solid-state electrolytes for lithium-ion batteries and other energy storage devices due to their high ionic conductivity and thermal stability.

**Sensor Technology:** Their chemical stability and ability to incorporate dopants make zinc-doped glasses suitable for various sensing applications, including gas sensors, humidity sensors, and biosensors.

**Sustainability:** Zinc-doped glasses offer potential as environmentally friendly alternatives to traditional materials in various applications, contributing to sustainability efforts and reducing environmental impact.

## 5.2 ADVANTAGES AND DISADVANTAGES

**Radiation Protection:** These glasses are specifically designed to attenuate harmful ionizing radiation, providing protection to individuals and sensitive equipment in environments with radiation exposure.

**Structural Integrity:** They offer both radiation shielding capabilities and structural support, making them suitable for applications where both properties are crucial, such as in nuclear power plants or medical facilities.

**Versatility:** Structural and radiation shielding glasses can be tailored to meet the specific requirements of different applications, allowing for customization of composition, thickness, and other properties.

**Durability:** These glasses are engineered to withstand harsh environmental conditions, including radiation exposure, temperature variations, and chemical corrosion, ensuring long-term performance and reliability.

**Safety:** By effectively attenuating ionizing radiation, these glasses help minimize the risk of radiation-related health hazards to personnel working in radiation-prone environments.

**Cost:** Developing and manufacturing glasses with specialized radiation shielding properties can be expensive due to the use of high-purity materials and precise manufacturing processes.

**Weight:** Depending on their composition and thickness, structural and radiation shielding glasses can be heavy, which may pose challenges in certain applications where weight is a concern. **Optical Properties:** Glasses designed for radiation shielding may have limited optical clarity or transparency, which can hinder visibility and monitoring of processes or equipment behind the glass.

**Maintenance:** Over time, structural and radiation shielding glasses may require maintenance or replacement due to wear and tear, surface damage, or degradation of shielding properties.

**Environmental Impact:** The production and disposal of specialized glasses may have environmental implications, particularly if they contain hazardous materials or require energy-intensive manufacturing processes. Proper disposal and recycling practices are essential to mitigate these concerns.

## REFERENCE

1. Sasirekha, C., Vijayakumar, M., & Marimuthu, K. (2023). Luminescence performance of Dy<sup>3+</sup> ions incorporated modifier reliant boro-tellurite glasses for white light applications. *Optik*, 289, 171268.  
<https://doi.org/10.1016/j.ijleo.2023.171268>.
2. Arivazhagan, S., Naseer, K. A., Mahmoud, K. A., Libeesh, N. K., Kumar, K. A., Kumar, K. C. N., ... & Khandaker, M. U. (2023). The radiation shielding proficiency and hyperspectral-based spatial distribution of lateritic terrain mapping in Irikkur block, Kannur, Kerala. *Nuclear Engineering and Technology*.  
<https://doi.org/10.1016/j.net.2023.06.008>.
3. Bassam, S. A., Naseer, K. A., Keerthana, V. K., Teresa, P. E., Sangeeth, C. S., Mahmoud, K. A., ... & Khandaker, M. U. (2023). Physical, structural, elastic and optical investigations on Dy<sup>3+</sup> ions doped boro-tellurite glasses for radiation attenuation application. *Radiation Physics and Chemistry*, 206, 110798.  
<https://doi.org/10.1016/j.radphyschem.2023.110798>.
4. Bassam, S. A., Naseer, K. A., Prakash, A. J., Mahmoud, K. A., SuchandSangeeth, C. S., Sayyed, M. I., ... & Khandaker, M. U. (2023). Effect of Tm<sub>2</sub>O<sub>3</sub> addition on the physical, structural, elastic, and radiation-resisting attributes of tellurite-based glasses. *Radiation Physics and Chemistry*, 209, 110988.  
<https://doi.org/10.1016/j.radphyschem.2023.110988>.
5. Teresa, P. E., Naseer, K. A., Padhi, R. K., El Shiekh, E., & Marimuthu, K. (2023). A comparative analysis on the spectroscopic qualities of modifiers and Sm<sup>3+</sup> ions integrated bismuth boro-tellurite glasses for visible orange appliances. *Optical Materials*, 143, 114272.  
<https://doi.org/10.1016/j.optmat.2023.114272>.
6. Ilik, E., Kavaz, E., Kilic, G., Issa, S. A., ALMisned, G., & Tekin, H. O. (2022). Synthesis and characterization of vanadium (V) oxide reinforced calcium-borate glasses: Experimental assessments on Al<sub>2</sub>O<sub>3</sub>/BaO<sub>2</sub>/ZnO contributions. *Journal of Non-Crystalline Solids*, 580, 121397.  
<https://doi.org/10.1016/j.jnoncrysol.2022.121397>.

7. Esawii, H. A., Salama, E., El-ahll, L. S., Moustafa, M., & Saleh, H. M. (2022). High impact tungsten-doped borosilicate glass composite for gamma and neutron transparent radiation shielding. *Progress in Nuclear Energy*, 150, 104321.  
<https://doi.org/10.1016/j.pnucene.2022.104321>.
8. Laariedh, F., Prabhu, N. S., Sayyed, M. I., Kumar, A., Alfadhli, S., & Kamath, S. D. (2021). Impact of replacement of B<sub>2</sub>O<sub>3</sub> by TeO<sub>2</sub> on the physical, optical and gamma ray shielding characteristics of Pb-free B<sub>2</sub>O<sub>3</sub>-TeO<sub>2</sub>-ZnO-Al<sub>2</sub>O<sub>3</sub>-Li<sub>2</sub>O-MgO glass system. *Optik*, 248, 168100.  
<https://doi.org/10.1016/j.ijleo.2021.168100>.
9. Issa, S. A., Tekin, H. O., Elsaman, R., Kilicoglu, O., Saddeek, Y. B., & Sayyed, M. I. (2019). Radiation shielding and mechanical properties of Al<sub>2</sub>O<sub>3</sub>-Na<sub>2</sub>O-B<sub>2</sub>O<sub>3</sub>-Bi<sub>2</sub>O<sub>3</sub> glasses using MCNPX Monte Carlo code. *Materials chemistry and physics*, 223, 209-219.  
<https://doi.org/10.1016/j.matchemphys.2018.10.064>.
10. Zaid, M. H. M., Matori, K. A., Nazrin, S. N., Azlan, M. N., Hisam, R., Iskandar, S. M., ... & Sayyed, M. I. (2021). Synthesis, mechanical characterization and photon radiation shielding properties of ZnO–Al<sub>2</sub>O<sub>3</sub>–Bi<sub>2</sub>O<sub>3</sub>–B<sub>2</sub>O<sub>3</sub> glass system. *Optical Materials*, 122, 111640.  
<https://doi.org/10.1016/j.optmat.2021.111640>.
11. Prabhu, N. S., Sayyed, M. I., Almuqrin, A. H., Khandaker, M. U., Mahmoud, K. A., Yasmin, S., & Kamath, S. D. (2022). Network-modifying role of Er<sup>3+</sup> ions on the structural, optical, mechanical, and radiation shielding properties of ZnF<sub>2</sub>–BaO–Al<sub>2</sub>O<sub>3</sub>–Li<sub>2</sub>O–B<sub>2</sub>O<sub>3</sub> glass. *Radiation Physics and Chemistry*, 200, 110228.  
<https://doi.org/10.1016/j.radphyschem.2022.110228>.
12. Arunkumar, S., Teresa, P. E., Marimuthu, K., Bassam, S. A., Silvia, D. J., Issa, S. A., ... & Alqahtani, M. S. (2023). Scrutinizing the physical, structural, elastic, optical and gamma ray shielding properties of Samarium ions infused Niobium Bariumtelluroborate glasses. *Radiation Physics and Chemistry*, 202, 110510.  
<https://doi.org/10.1016/j.radphyschem.2022.110510>.
13. Poojha, M. K., Vijayakumar, M., Bassam, S. A., Sayyed, M. I., Marimuthu, K., Alqahtani, M. S., & El Shiekh, E. (2023). Comprehensive assessment of radiation

- shielding properties of novel multi-component lead boro-tellurite glasses. *Radiation Physics and Chemistry*, 206, 110811.  
<https://doi.org/10.1016/j.radphyschem.2023.110811>.
14. A.F.A. El-Rehim et.al, Structural, Elastic Moduli, and Radiation Shielding of SiO<sub>2</sub>- TiO<sub>2</sub>-La<sub>2</sub>O<sub>3</sub>-Na<sub>2</sub>O Glasses Containing Y<sub>2</sub>O<sub>3</sub>, *J. Mater. Eng. Perform.* 30 (2021) 1872–1884.  
<https://doi.org/10.1007/s11665-021-05513-w>.
  15. M.G. Dong et.al, Investigation of gamma radiation shielding properties of lithium zinc bismuth borate glasses using XCOM program and MCNP5 code, *J. Non. Cryst. Solids.* 468 (2017) 12–16.  
<https://doi.org/10.1016/j.jnoncrysol.2017.04.018>.
  16. K. A. Naseer et.al, Impact of Bi<sub>2</sub>O<sub>3</sub> modifier concentration on barium–zinc borate glasses: physical, structural, elastic, and radiation-shielding properties, *Eur. Phys. J. Plus* (2021) 136:116,  
<https://doi.org/10.1140/epjp/s13360-020-01056-6>.
  17. E. Şakar et.al, Phy-X / PSD: Development of a user friendly online software for calculation of parameters relevant to radiation shielding and dosimetry, *Radiat. Phys. Chem.* 166 (2020) 108496.  
<https://doi.org/10.1016/j.radphyschem.2019.108496>.
  18. Y.S. Rammaha et.al, Role of ZnO on TeO<sub>2</sub>.Li<sub>2</sub>O.ZnO glasses for optical and nuclear radiation shielding applications utilizing MCNP5 simulations and WINXCOM program, *Journal of Non-Crystalline Solids* 544 (2020) 120162,  
<https://doi.org/10.1016/j.jnoncrysol.2020.120162>.
  19. K.A. Naseer et.al, The concentration impact of Yb<sup>3+</sup> on the bismuth boro-phosphate glasses: Physical, structural, optical, elastic, and radiation-shielding properties, *Radiation Physics and Chemistry* 188 (2021) 109617,  
<https://doi.org/10.1016/j.radphyschem.2021.109617>.
  20. Al-Buriah, M. S., Eke, C., Alomairy, S., Mutuwong, C., & Sfina, N. (2021). Micro- hardness and gamma- ray attenuation properties of lead iron phosphate glasses. *Journal of Materials Science: Materials in Electronics*, 32(10), 13906-13916.